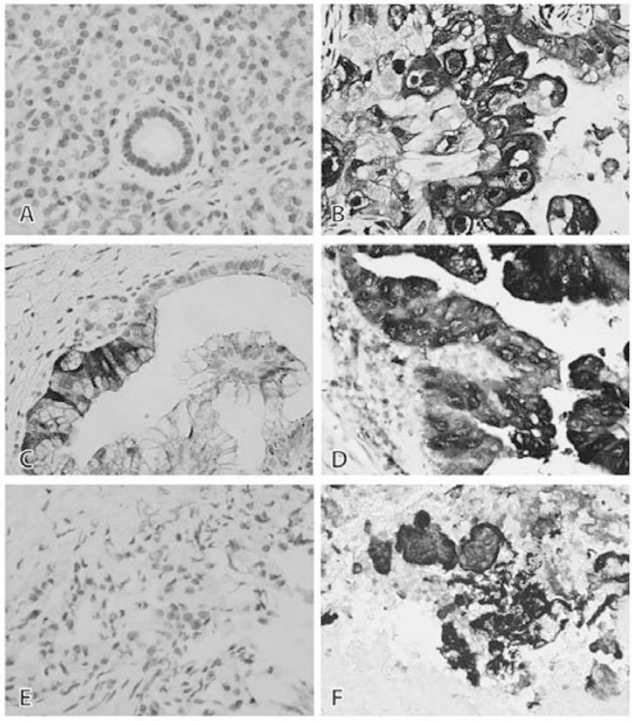

1880 Immunohistochemical Markers and Prognosis with Pancreatic Neuroendocrine Tumors

Z Zhao, MJ Mentrikoski, TW Bauer, JM Lindberg, EB Stelow. University of Virginia Health System, Charlottesville, VA.

Background: Pancreatic neuroendocrine tumors (PanNETs) exhibit a broad range of clinical behavior. However, there are few histological features or other markers to aid pathologists in assessing prognosis. We investigated a series of possible prognostic markers and compared them to outcome for a large series of PanNETs.

Design: 81 cases of resected primary PanNETs were retrieved from our pathology database and the clinical histories reviewed. A tissue microarray was constructed and analyzed with immunohistochemical (IHC) stains, including cytokeratin 19 (CK19), progesterone receptor (PR), CD117, PAX8, Ki-67, HBME1, and CD10. Interpretation of Ki-67 was based on the WHO grading system as 0 (negative), 1 (<2% of nuclei staining), 2 (3-20%) and 3 (>20%). Other markers were considered positive if >5% of tumor cells stained.

Results: The IHC results are summarized in the table below.

Immunohistochemical Analysis of PanNETs

	Ki-67 index >2%	CK19	PAX8	PR	CD10	HBME1	CD117
LN metastasis at surgery (n=21)	4 (19%)	13 (62%)	8 (38%)	8 (38%)	4 (19%)	3 (14%)	3 (14%)
No LN metastasis at surgery (n=60)	5 (8%)	28 (47%)	40 (67%)	35 (58%)	13 (22%)	1 (2%)	3 (5%)
P-value	0.2279	0.3116	0.0375	0.1324	1.000	0.0516	0.1768
EM at surgery (n=14)	4 (29%)	10 (71%)	5 (36%)	6 (43%)	2 (14%)	2 (14%)	2 (14%)
No EM at surgery (n=67)	5 (7%)	31 (46%)	43 (64%)	36 (54%)	15 (22%)	3 (4%)	4 (6%)
P-value	0.0435	0.1405	0.0721	0.5612	0.7227	0.2043	0.2759
Recurrence (n = 17)	3 (18%)	10 (59%)	7 (41%)	10 (59%)	3 (18%)	2 (12%)	2 (12%)
No recurrence (n = 64)	6 (9%)	30 (47%)	40 (63%)	32 (50%)	13 (20%)	3 (5%)	4 (6%)
P-value	0.3877	0.4241	0.1666	0.5917	1.000	0.2808	0.6006
No metastasis at surgery with recurrence (n = 9)	1 (11%)	4 (44%)	5 (56%)	6 (67%)	2 (22%)	0 (0%)	0 (0%)
No metastasis at surgery and no recurrence (n=44)	4 (9%)	19 (43%)	32 (73%)	26 (59%)	10 (23%)	2 (5%)	3 (7%)
P-value	1.000	1.000	0.4274	1.000	1.000	1.000	1.000

More cases with extranodal metastasis (EM) at surgery compared to those without had recurrent disease (50 vs 15%, p=0.0077), but LN metastasis alone at surgery did not predict recurrent disease (33 vs 17%, p=0.1262). Importantaly, no marker predicted recurrent disease for tumors without metastasis (stage I and IIA) at surgery.

Conclusions: Our study confirmed previous studies, showing tumor grade, Ki-67 index, PAX8 and HBME1 staining predict stage at time of resection. Presence of EM at surgery is predictive of disease recurrence. Nonetheless, these markers, including the Ki-67 index, seem to be of limited use for predicting which stage I and IIA PanNETs will eventually recur.

Pathobiology

1881 Discriminating Uterine Serous Carcinoma from High Grade Ovarian and Fallopian Tube Serous Carcinoma by Whole Genome Expression

QF Ahmed, S Bandyopadyay, B Alosh, E AbdulFatah, S Barak, G Dyson, A Bollig-Fischer, R Ali-Fehmi. Wayne State University, Detroit, MI; Karmanos Cancer Institute, Detroit, MI.

Background: The morphologic and molecular similarities amongst uterine serous carcinoma (USC), high grade ovarian serous carcinoma (OSC) and fallopian tube serous carcinoma (FTSC) are well known. The aim of our study was to analyze and highlight the differences at the molecular level.

Design: We retrieved 24 cases of primary high grade OSC (n=8), FTSC (n=8) and USC (n=8) age and stage matched from our pathology database. We measured whole-genome mRNA expression in all formalin-fixed paraffin (FFPE) specimens. Total RNA was isolated and RNA quantity was estimated using a NanoDrop 1000 spectrophotometer. Further sample processing and gene expression profiling was done using an Illumina Human Whole-Genome HT Assay kit. A total of 29,000 annotated genes derived from RefSeq were measured. A t-test determined significant differential gene expression.

Results: High grade (OSC) and (FTSC) did not show any significant difference in mRNA expression supporting the concept of similar cell of origin and development pathway in both. At the same time USC was distinct. 1,740 genes were differentially expressed ($p<.05$) for both uterine versus ovarian and uterine versus fallopian cancer comparisons. A pathway impact analysis of the resulting gene set indicated significant pathway-level differences, listed in Table 1.

Pathway name	Impact factor	#Genes in pathway	#Input genes in pathway	#Pathway genes on array	p-value
Cell adhesion molecules (CAMs)	122.391	134	22	134	2.40E-04
Leukocyte transendothelial migration	106.673	119	20	119	3.29E-04
Antigen processing and presentation	41/528	89	3	89	0.960
ECM-receptor interaction	27.573	84	27	84	5.00E-12
Phosphatidylinositol/PLC signaling system	26.366	76	10	76	0.046
Focal adhesion	25.203	203	43	203	1.21E-10
Calcium signaling pathway	11.25	182	27	182	2.85E-04
Gap junction	10.625	96	16	96	0.001
Tight junction	10.411	135	22	135	2.67E-04
GnRH signaling pathway	7.068	103	16	103	0.003
Adherens junction	6.924	78	11	78	0.024
TGF-beta signaling pathway	6.758	87	13	87	0.009
Insulin signaling pathway	6.735	138	19	138	0.005
MAPK signaling pathway	6.527	272	30	272	0.014

Table 1. Enriched pathways and their significance according to pathway level analysis using Onto-tool pathway express

Conclusions: Understanding molecular differences between these diseases might help in identifying some of the clinical differences, prognostic biomarkers and targeted treatment to improve USC outcomes.

1882 Progesterone Induces NF-kB Activation through PI3K/Akt-2 Signal Pathway Dependent of Heterotrimeric Gi/Go Proteins in MCF-7 Breast Cancer

F Candanedo-Gonzalez, P Cortes-Reynosa, N Serna-Marquez, S Villegas-Comonfort, R Espinoza-Neira, A Soto-Guzman, E Perez-Salzar. CINVESTAV, Mexico City, DF, Mexico.

Background: Around 75% of breast tumors are positive for the progesterone receptor (PR). Less than 10% of estrogen receptor-negative (ER-) breast cancers are progesterone receptor-positive (PR+), which most often affects women under 50 years of age with high-grade tumors with more aggressive behavior. However, the signal transduction pathways activated by progesterone have not been studied in detail.

Design: Objective: To better understand the role of the rapid non-genomic signalling effects of progesterone, we investigated the mechanisms leading to NF-kB activation.

Methods: MCF-7 and MDA-MB-231 breast cancer cells were cultured in DMEM and were serum-starved for 12 h before treatment with inhibitors (PTX, Wortmaninn, Rapamycin, A6730 Akt-1/2 kinase inhibitor, PP2, PP3) and/or progesterone (100 nM) for 30 min and evaluated by Western blot. Statistical analysis: Results are expressed as mean ± SD. Data was statistically analyzed using one-way ANOVA. Statistical probability of $p < 0.05$ was considered significant.

Results: Stimulation of MCF-7 cells with progesterone induced the rapidly NF-kB activation, in a time and concentration-dependent manner. The inhibition with PTX, Wortmaninn, Ag730 and PP2 completely prevent the NF-kB activation. These results showed that the mechanism of NF-kB activation induced by progesterone is dependent of heterotrimeric Gi/Go proteins, c-Src, and PI3K/Akt-2 signaling pathways.

Conclusions: This is the first study to show that progesterone stimulates the NF-kB activation through PI3K/Akt-signal pathway dependent of heterotrimeric Gi/Go proteins in MCF-7 breast cancer cells. Understanding the role of the progesterone and its receptor in breast cancer, will allow to offer new therapeutic options in the future.

1883 Elevated YB-1 Expression Is Associated with Cancer Progression and EMT Markers in Breast Tumors

B Castellana, M Aizpurua, I Sansano, V Peg, S Ramon y Cajal. Molecular Pathology, Vall d'Hebron Research Institute, Autonomous University of Barcelona, Barcelona, Spain; Vall d'Hebron University Hospital, Barcelona, Spain.

Background: Y box binding protein-1 (YB-1) is a multifunctional oncoprotein up-regulated in several cancers. When YB-1 is activated by phosphorylation on S102 it is relocated to the nucleus where it can be involved in the transcriptional activation of genes implicated in growth, drug resistance, migration and invasion. YB-1 has been reported to be involved in the activation of an Epithelial to Mesenchymal Transition (EMT) program. The acquisition of EMT features aids tumor invasion and further metastasis. We aim to investigate the correlations between YB-1 expression and EMT factors in a panel of breast tumors as well as the presence of this oncoprotein in lymph node metastasis.

Design: 77 FFPE blocks of breast tumors were grouped according to their subtype: 32,5 % HR+/HER-2-/ low Ki67 (Lum A-like), 28,6 % ER+/HER2-/high Ki67 or PR low (Lum B-like, HER2-), 18,2 % 3,9% ER+/HER2+(LumB-like, HER2+), 2,6 % HER2+ (HER2 positive, non-luminal) and 13 % HR-/HER2- (Triple negative). Immunohistochemical analysis of YB-1 and its phosphorylated form was performed. The expression of EMT markers such as Snail1, Slug, N-Cadherin, VEGF and proteins from the TGFβ pathway (pSmad2 and Smad2/3) was analyzed by Western Blotting.

Results: By immunohistochemistry, YB-1 is highly express in high grade tumors (P = 0.043) and especially in Her2 and triple negative tumors (P= 0.003). Moreover, pYB-1 correlates positively with N-Cadherin membrane staining (0.027; P =0,026). Analysis by Western Blotting showed positive Spearman's correlations between YB-1 and Snail (0,337; P =0,015) and Slug (0,226; P =0,038). Similar results were obtained with the phosphorylated YB-1 form (pYB-1) that also correlates with Snail1 (0,601; P =0,002), Slug (0,654; P =0,003) and Smad2/3(0,689; P =0,002). Interestingly, we found a significant high expression of pYB-1 and more striking of pYB-1 found stained exclusively in the nucleus of lymph node metastasis with an elevated expression in patients with >9 positive lymph nodes (pN3) ($P < 0.05$).

Conclusions: We show that YB-1 expression, which is highly up-regulated in aggressive tumors (Grade 3, TNBC) compared to luminal tumors, positively correlates with EMT markers. This correlated expression is even higher in the case of the YB-1 phosphorylated form, suggesting that its nuclear localization is implicated in the acquisition of EMT-like features. Further studies are currently ongoing in breast cancer cell lines in order to decipher the role of YB-1 in cancer progression.

1884 Evaluation of Mutation Patterns in Microsatellite Instability-High Colorectal Cancers Using a 50 Gene Cancer Panel

AM Cushman-Vokoun, SA Rapp. University of Nebraska Medical Center, Omaha, NE.

Background: Microsatellite Instability-High (MSI-H) colorectal carcinomas (CRCs) may be associated with germline mutation in genes encoding Mismatch Repair (MMR) enzymes or sporadic methylation of the *MLH1* promoter. Defective MMR results in a mutator phenotype in CRC. Some studies have suggested a predisposition for G>A transition mutations with MMR deficiency. Investigating patterns of mutation in multiple genes using Next Generation Sequencing (NGS) will likely further the understanding of MSI-H CRCs with regard to therapy.

Design: DNA extracted from 18 cases of formalin-fixed paraffin embedded MSI-H CRC was analyzed using the 50 gene Ion AmpliSeq™ Cancer HotSpot Panel v2. Barcoded libraries were constructed and clonal amplification and enrichment of template-positive Ion Sphere Particles™ (ISPs) was performed using the Ion OneTouch™ 2 system. Sequencing of ISPs was performed using the Ion Personal Genome Machine (PGM)™ and the data was analyzed using the Ion Torrent Server Variant Caller Software v.3.4.4 and the Integrative Genomics Viewer (IGV). Analysis of corresponding normal tissue and dideoxy sequencing were used to verify somatic mutations. Only single nucleotide variants (SNVs) were included in the analysis.

Results: The average number of somatic SNVs per tumor was 3 and the total number of SNVs was 55. Forty-nine non-synonymous (NS) (89%), 3 synonymous (5%) and 3 non-coding (5%) SNVs were identified. Of these, there were 17 G>A mutations in the sense strand and 14 G>A mutations in the antisense strand (56%). Of the NS SNVs, arginine was the most commonly substituted amino acid (35%). In the 18 cases, *BRAF* (61%), *PIK3CA* (28%), *KRAS* (22%), *TP53 (22%)* and *FBXW7* (22%) were the most commonly mutated genes. All *FBXW7* mutations were G>A transitions on the sense or antisense strand, resulting in arginine mutations. All *KRAS* mutations were G>A transitions (c.35G>A or c.38G>A) in the sense strand, resulting in glycine mutations.

Conclusions: NGS using a 50 gene cancer panel is useful in the identification of mutation patterns in MSI-H CRCs. G>A transition mutations are prevalent in MSI-H tumors. As a result, there is a preponderance of NS mutations involving arginine replacement, especially in the gene *FBXW7*. Proteins containing important arginine residues, such as *FBXW7,* should be further evaluated in MSI-H tumors. Similar to a few studies, *KRAS* mutations in MSI-High tumors are predominantly G>A (p.G12D or p.G13D) mutations. The above findings should be studied in microsatellite stable tumors to further clarify their significance.

1885 Genetic Intratumoral Heterogeneity Revealed by Deep Sequencing in Her2 Amplified Stomach Cancer

J Deeds, E Orlando, A Raza, S Weng, Y Shim, H Bitter, R Leary, S Mahan, M Palmer, W Winckler, R Mosher. Novartis, Cambridge, MA.

Background: Pre-existing genetic heterogeneity is a common feature of numerous cancers. The presence of clonal populations with different amplifications of oncogenes or tumor suppressors could explain sensitivity and resistance to targeted therapies. In order to discover regionally defined known and unknown genetic amplifications or deletions, we employed deep sequencing of dissected regions of stomach cancer.

Design: Two FFPE primary stomach cancer samples (cases 373 and 377) known to be amplified for Her2 were examined. 3.5um sections were stained by IHC for Her2 and FGFR2 protein. Each sample was cut into 3mm 'cubes' of tissue (regions) and total genomic DNA was extracted from each. Seven regions from case 377 and five regions from case 373 were selected for exome sequencing at 300x coverage. One region with low tumor content from each case was used as a control. In addition, DNA from 28 regions from case 377 were pooled and analyzed.

Results: Case 377: Of the five regions examined, one was found to be amplified for FGFR2 and was also g FGFR2 positive tumor cells. All five regions demonstrated amplification for Her2. Four of the five regions contained a large proportion of IHC Her2 positive tumor cells. One region only contained a small focus of Her2 positive tumor cells and a larger number of Her2 negative tumor cells. Three of five regions were found to be amplified for both CCND1 and MYC. FGFR2 and CCND1 were not found to be amplified in the pooled DNA sample, suggesting that these amplifications would be missed in a whole tumor extraction. Case 373: None of the three regions were amplified for FGFR2 and were all negative by IHC for FGFR2. The two regions which were Her2 positive by IHC were found to be amplified for Her2 as well as MYC. The other region was not amplified for either gene and did not express Her2 protein. CDKN2A was found to be deleted in all three regions.

Conclusions: Deep sequencing of regionally dissected FFPE samples is technically feasible and can identify regionally distinct amplifications. Cluster analysis of the exome sequencing data may reveal features of branched tumor evolution. Exome sequencing of entire tumor samples may miss regionally amplified or deleted genomic sites. Co-amplification of multiple genes in tumor foci cannot be determined from whole samples. Our data show that some regions have co-amplifications of two or more genes and some have mutually exclusive amplifications. These may affect the selection of appropriate therapies for individual patients.

1886 Loss of *PTEN* Is a Common Event Involved in Colitis-Induced Mucinous Carcinoma in Mice and in Humans

T DeJulio, K Ma, B Shetuni, H Li, J Liao, G-Y Yang. Northwestern University, Chicago, IL.

Background: *PTEN* has been identified as a tumor suppressor gene that is mutated in a large number of cancers at a high frequency, including colon. Functionally, it negatively regulates intracellular levels of IP3-phosphatase and the Akt/PKB signaling pathway. Whether or not *PTEN* mutation plays a role in the development of colitis-induced mucinous carcinoma is not known.

Design: To study the role of *PTEN* in colitis-induced colorectal carcinogenesis, the development of colorectal carcinoma was studied using DSS-induced colitis-carcinogenesis in *PTEN* -deficient mice. Female wild-type C57BL/6 ($PTEN^{+/+}$) and $PTEN^{+/-}$ mice were administered 0.7% DSS (w/v) through their drinking fluid for 12 DSS cycles. Swiss-roll embedded mice colon sections were analyzed histopathologically and immunohistochemically for the grading of colitis and development of dysplasia and carcinoma with established criteria. In addition, a total of 26 human colorectal mucinous carcinomas queried from the Surgical Pathology Division of the Department of Pathology of Northwestern University were examined by immunohistochemistry for *PTEN* expression.

Results: Colorectal inflammation and mucosal ulceration of mild severity were observed in both $PTEN^{+/+}$ and $PTEN^{+/-}$ mice. Three of 8 (37.5%) $PTEN^{+/+}$ mice developed colorectal tumors after 12 DSS cycles, with a tumor volume 130.8 ± 9.28 mm^3 (mean ± SE). In $PTEN^{+/-}$ mice, significantly increased tumor development was observed, in that 12 of 18 (66.7%) mice developed colorectal tumors with a higher tumor volume of 467 ± 28.3 mm^3 ($p<0.01$). Histopathologically, the tumors were confirmed to be well-differentiated mucinous adenocarcinomas. Immunohistochemical analysis revealed that the colonic epithelial cells in $PTEN^{+/-}$ mice displayed a significant increase of phosphorylated AKT and beta-catenin (S552)-labeled colonic progenitor cells. *PTEN* immunostaining for human colonic mucinous carcinoma showed that *PTEN* expression was confined to the cytoplasm of carcinoma cells as a dark brown staining pattern. Loss of *PTEN* expression was found in 9 of 26 (34.6%) mucinous carcinomas.

Conclusions: Loss of *PTEN* is a common genetic event in human invasive mucinous adenocarcinoma, and *PTEN* knockout increases susceptibility to colitis-induced mucinous carcinoma development in mice. These results imply that *PTEN* and its regulated pathway can be a useful malignant biomarker for colonic mucinous carcinoma and serve as potential molecular target for prevention and therapy.

1887 AREG Expression Is Associated with Poor Survival of Lung and Gastric Adenocarcinoma

Q Ding, M Esebua, S Wang, J Xia. University of Missouri, Columbia, MO; Tongji Medical College, Wuhan, China.

Background: Amphiregulin (AREG) is a member of the EGFR family and functions as an autocrine growth factor and a mitogen, which can interact with the EGF/TGF-alpha receptor to promote cell growth. The tumor microenvironment includes tumor cells, the surrounding fibroblasts, immune cells, signaling molecules, and the extracellular matrix. Regulatory T cells (Tregs) are a component of the immune system in tumor microenvironment that suppress immune reaction and facilitate tumor development and progression.

Design: We collected 75 lung and 90 gastric adenocarcinoma with clinical information, examined the expression of AREG by IHC, and then analyzed its expression with tumor stage and prognosis. We also collected matched blood and malignant pleural or peritoneal effusion from lung or gastric adenocarcinoma patient (7 cases each), and then analyzed AREG expression by ELISA and compared to the blood samples from healthy individuals.FACS has also been performed to evaluate the CD4+/CD25+/Foxp3+ Treg cells in peripheral blood and malignant pleural and peritoneal fluid.

Results: The IHC result showed that AREG was expressed at high levels in 48 of 75 lung adenocarcinoma and 52 of 90 gastric adenocarcinoma, and AREG expression was associated with tumor size and lymph node metastasis in gastric adenocarcinoma (Figure 1A). Importantly, AREG expression was also associated with overall poor survival of both lung and gastric cancers (Figure 1B). In addition, the AREG levels were markedly elevated in blood, tumor tissue, and pleural and peritoneal effusion in lung and gastric adenocarcinoma (Figure 1C). FACS revealed that number of CD4+/CD25+/Foxp3+ Treg cells was increased in tumor-derived effusion and peripheral blood , if compared to peripheral blood mononuclear cell of the healthy controls (Figure 1D). The co-incidence of increased level of both AREG and Treg cells might indicate a potential relationship between Treg and AREG.

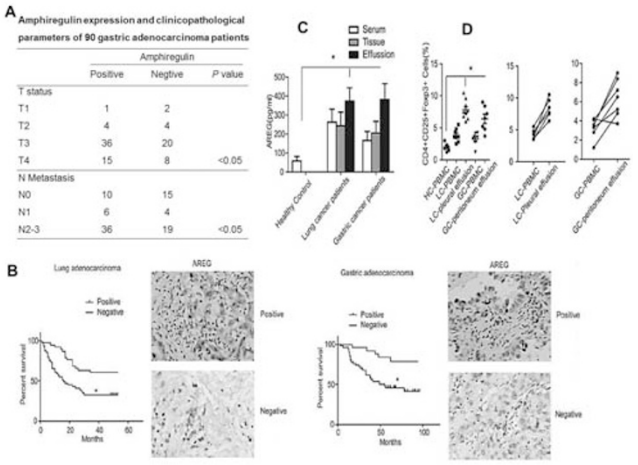

Conclusions: AREG was highly expressed, and associated with poor survival in lung and gastric adenocarcinoma patients, indicating that it may be a poor prognosis marker. AREG may regulate Treg through EGFR and its downstream signaling, which lead to tumor development and progression.

1888 Characterization of Human Subtype-Specific Macrophage Markers

E Forgo, RJ Marinelli, J Odegaard, M van de Rijn. Stanford University School of Medicine, Stanford, CA.

Background: Macrophages are an integral part of the tumor microenvironment where, depending on tumor type, they can have a different effect on clinical outcome. Most of our knowledge regarding macrophage subtypes has come from *in vitro* murine research, with little contribution from *in vivo* human tissue and disease. The M1 and M2 subtypes described in murine macrophages are difficult to replicate in humans. In an attempt to define human macrophage subtype-specific markers, we performed a large-scale characterization of 9 different disease entities and normal tissues with 14 FFPE-compatible antibodies that are known to react with macrophages.

Design: A tissue microarray (TMA) was constructed with 0.6mm cores from 54 cases of human FFPE tissue from 9 different diseases, that included endometriotic cyst, foreign body giant cell reaction, gout, non-specific sinus histiocytosis, rheumatoid nodule, sarcoid, xanthogranuloma, xanthogranulomatous inflammation, and xanthoma. Normal lymph nodes, spleen, colon and breast tissue were also included. Immunohistochemistry was performed on serial sections with 14 antibodies, the TMA was scanned into digital images and the staining patterns were compared using a new display function in the Stanford Tissue Microarray Database that allows simultaneous inspection of multiple images. The antibodies studied were: CD1a, CD4, CD14, CD31, CD33, CD43, CD45RO, CD68, CD123, CD163, CD300c, Langerin, S100P, and TCL1a.

Results: Of the 14 antibodies tested, 8 (CD14, CD31, CD33, CD43, CD68, CD123, CD163, CD300c) showed non-overlapping reaction patterns in pair-wise comparisons with regards to macrophage staining and/or specific localization within the tissues. One example was the staining of all multinucleated giant cells by CD68 in a foreign body giant cell reaction, but incomplete staining of the same giant cells by CD163. Another example showed distinctive macrophage subsets stained by CD14, CD68 and CD163 in duodenal xanthogranulomatous inflammation.

Conclusions: In mice, different functional subtypes of macrophages have been described, but in humans no systematic study to define macrophage diversity has been performed. The broad range of human disease offers an opportunity to study macrophages in different environments not recognized in mice. We compared 14 antibodies across 9 human diseases and normal tissue and at this initial phase, identified markers that recognized distinct subsets of macrophages. Further integration of this data with an additional 24 FFPE-compatible macrophage markers may lead to the recognition of human macrophage subsets by differentiation markers.

1889 Molecular and Immunohistochemical Profiling of Leiomyosarcomas

MP Gailey, NV Guseva, MM Milhem, BJ Miller, MR Miller, AM Bellizzi, MD Henry, D Ma. University of Iowa Hospitals and Clinics, Iowa City, IA.

Background: Leiomyosarcoma (LMS) is an aggressive tumor with high recurrence and metastatic rate. No efficacious therapy is available once it becomes systemic. LMSs have complex genomics and lack clinical and molecular predictors of outcome. Comprehending the most dysregulated pathway(s) may lead to novel therapeutic options. We employed the next generation sequencing (NGS) to search for mutations and examined the expression of two tumor suppressors, PTEN and dystroglycan (DG), and the metastatic suppressor NM23H1 by immunohistochemistry (IHC) in human LMSs.

Design: Thirty high grade LMSs, 10 each from the limb, retroperitoneum and uterus, were selected from tissue archives. Genomic DNA was isolated from paired formalin-fixed, paraffin-embedded tumor and normal tissues using the DNA Mini Extraction kit (Qiagen, Valencia, CA) and analyzed by NGS using the Ion AmpliSeq™ Cancer Hotspot Panel v2 (Life Technologies, Carlsbad, CA). The same tumor blocks for NGS were used for PTEN, DG, and NM23H1 IHC and the expression was scored using a 3-tier system: Positive (≥90% of cells intensely positive); Reduced (regional positivity with≥10% of cells negative and/or decreased intensity of staining); Loss (≤1% of cells positive).

Results: PTEN expression was lost or reduced in 57% of the cases, with the highest frequency in LMS of the limb (80%), followed by uterus (60%) and retroperitoneum (30%). Loss/reduction of DG was seen in 40% of tumors. All limb and uterine tumors with DG loss/reduction had concurrent PTEN loss. The highest rate of NM23H1 loss/reduction was seen in the retroperitoneal LMSs (5/10). NGS analysis of the limb and uterus tumors identified mutations in the *TP53* gene in 35% of the tumors (4 in limb and 3 in uterus; n=20) and *ATM* mutations in 3 others. *PTEN*, *Rb* and *MET* mutations were also seen.

IHC and NGS profiling of LMS

	Number of cases with loss or reduced expression by IHC				NGS
Location	DG	PTEN	NM23H1	Concurrent DG/ PTEN loss	Mutations
Limb	6	8	2	6	TP53 (4), ATM (1), Rb (1)
Uterus	4	6	2	4	TP53 (3), ATM (2), PTEN (1), MET (1)
Retroperitoneum	2	3	5	0	In process
Total (%)	12 (40)	17 (57)	9 (30)	10 (33)	

Conclusions: Loss/reduced PTEN expression was frequent in LMS (57%). All limb and uterine LMS with DG loss showed concurrent loss/reduction of PTEN. Loss of NM23H1 was most frequent in retroperitoneal tumors. The most frequently mutated genes are: *TP53* (35%; n=20) and *ATM* (15%; n=20). Frequent PTEN loss and *TP53* mutations in LMSs may have implications for targeted therapies. Loss of DG and NM23H1 may have prognostic value. NGS analysis on the retroperitoneal LMSs is in process.

1890 *MCL1* Gene Amplification Is Associated with MCL-1 Overexpression in Triple Negative Breast Cancer

J Giltnane, J Balko, MG Kuba, L Schwarz, M Sanders, V Sanchez, J Pinto, F Doimi, H Gomez, J Ross, G Palmer, R Yelensky, M Cronin, V Miller, P Stephens, R Cook, C Arteaga. Vanderbilt University, Nashville, TN; Oncosalud, Lima, Peru; Instituto Nacional de Enfermedades Neoplásicas, Lima, Peru; Foundation Medicine, Cambridge, MA.

Background: *MCL1* (1q21) encodes a mitochondrial protein which inhibits apoptosis through sequestration of the pro-apoptotic protein Bak. Frequent *MCL1* copy number alterations (CNAs) are present in solid tumors; this may be a biomarker of response to MCL-1 targeted therapies in development. Through a next-generation sequencing (NGS) study of triple negative breast carcinomas (TNBCs) treated with neoadjuvant chemotherapy, we discovered a frequent rate of *MCL1* CNAs. We hypothesized that this would lead to protein overexpression, and sought to compare immunohistochemistry (IHC) to NGS results.

Design: Tissue microarrays were constructed from FFPE tumor blocks representing a cohort of 111 TNBC tumor samples from patients diagnosed and treated with neoadjuvant chemotherapy at the Instituto Nacional de Enfermedades Neoplásicas in Lima, Perú and retrieved from hospital archives under an institutionally approved protocol. DNA had been previously extracted from the same samples for targeted NGS by the FoundationOne™ assay. Following IHC detection of MCL-1 protein, digital intensity scores were determined in residual tumor cells selected by two breast pathologists using an Ariol automated system.

Results: *MCL1* amplification was present in 40 of 81 tumors with available CNA results and associated with MCL-1 overexpression as a continuous variable of total normalized intensity (p=0.01). This result is consistent with published concordance of *MCL1* CNAs with *MCL1*mRNA expression in The Cancer Genome Atlas (TCGA). However, high MCL-1 protein levels in the absence of detected CNAs were also detected, suggesting alternative mechanisms of overexpression. However, our post-NAC cohort harbored a significantly higher rate of*MCL1* CNAs when compared to subtype-matched untreated primary tumors in that cohort (54% in post-NAC TNBC vs. 19% in TCGA basal-like tumors; p=0.0006).

Conclusions: We have observed a direct correlation between *MCL1* gene amplification and protein overexpression in a large cohort of TNBCs. Thus IHC may be a rapid, economical assay for prediction of response to MCL-1 targeted inhibitors. We propose that MCL1 overexpression is associated with *de novo* resistance to chemotherapy and therefore enriched in residual tumors post neoadjuvant treatment. Additional studies are underway to compare IHC and FISH as companion diagnostic assays in this setting.

1891 Platelet-Modulation of Natural Killer Cell Reactivity on Cancer Cells

N Glaviano, CD Spillane, NM Cooke, B Ffrench, S O'Toole, D Kenny, C Gardiner, O Sheils, JJ O'Leary. Trinity College Dublin, Dublin, Ireland; The Coombe Women & Infants University Hospital, Dublin, Ireland; DCU, Dublin, Ireland; RCSI, Dublin, Ireland.

Background: Tumour metastasis is a pivotal factor in determining adverse prognostic outcome for cancer patients. Dissemination of circulating tumour cells (CTCs) from a primary tumour is necessary for the establishment of metastases. Natural Killer (NK) cells are cytotoxic lymphocytes, which play a major role in anti-tumour immunity.

Thus, for CTCs to efficiently establish a metastasis, they must evade active immune surveillance and lysis by NK cells. Previously we described the ability of platelets to adhere or 'cloak' cancer cells, imparting a prosurvival signal on them. Since activated platelets can directly inhibit NK cells, we postulate that platelet cloak formation is critical to the NK cell's inability to effectively lyse CTCs. The present study focuses on this tumour-platelet-NK cell interaction, investigating the effects of platelets in modulating NK cell reactivity on cancer cells.

Design: The lung squamous carcinoma SK-MES-1 and myelogenous leukemia K562 cell lines were used in this study. Platelets were co-incubated with cancer cells (1/1000 ratio) for 1 minute to allow platelet-coating. LymphoPrep was carried out to isolate Peripheral Blood Mononuclear Cells (PBMCs). NK cell activity was detected using the CD107a assay and quantified by flow cytometry.

Results: 70% and 51% direct platelet adhesion was detected on SK-MES-1 cells and K562 respectively. There was a statistically significant reduction of 33% and 53% ($p \leq 0.01$) in NK cell activity when compared to control SK-MES-1 and K562 cells, respectively. To further investigate the mechanism of action, we separated the platelet coated cells from the releasate produced upon platelet activation by SK-MES-1 cells. There was no decrease in NK cell activity with the pure platelet coated cells. However, there was a significant 35% reduction ($p<0.01$) with the platelet releasate. Preliminary data from the K562 cells has demonstrated a strongly correlated with that of the SK-MES-1.

Conclusions: Our *in vitro* data indicates that one mechanism by which platelets contribute to metastasis is by impeding NK cancer cell-elimination of tumour cells. Furthermore, that the releasate from tumour cell activated platelets is responsible for this inhibition of NK immuno-surveillance.

1892 Clonal Evolution of Cancer Examined *Via* Next-Generation Sequencing of 266 Paired Primary and Metastatic Tumors

RS Goswami, KP Patel, KD Aldape, RR Singh, KJ Jabbar, S Kopetz, RH Alvarez, MA Davies, V Subbiah, KR Shaw, F Meric-Bernstam, R Luthra, MJ Routbort. UT MD Anderson Cancer Center, Houston, TX.

Background: Next-generation sequencing (NGS) allows for examination of tumoral subclones, assessing heterogeneity and tumoral evolution. To date, studies addressing clonal evolution using NGS have been limited to small patient cohorts. We report here findings of concordance and discordance in NGS mutational profiles in a large series of well-characterized primary/metastasis tumor pairs.

Design: DNA isolated from fixed, paraffin-embedded primary and metastatic tumor pairs was analyzed using a clinically validated 46-gene cancer mutation hotspot assay on the Ion Torrent PGM (Life Technologies). Primary tumors included colorectal (32%) and breast carcinomas (30%), melanoma (7%), and other sites (31%). A combination of vendor (TorrentSuite 2.0, Life Technologies) and custom (OncoSeek, UT MD Anderson) software for filtering, annotation, and sample comparison was used. Mutation call cutoffs were set at an allelic frequency of 5%. For each sample pair, tumor percentage, mutational allelic frequency, time interval between onset of primary tumor and metastasis, and presence/absence of neoadjuvant therapy were obtained.

Results: 213 (80%) of 266 pairs showed identical genetic profiles. This included a predominant group of tumors with defining somatic mutation signatures (146, 55%), as well as a subset with no mutations (67, 25%). 53 pairs (20%) showed≥1 novel mutation(s) between the primary and metastasis. Of these, 4 pairs (2%) showed mutations in the metastasis and not the primary, but were associated with primary neoadjuvant chemotherapy. In 10 pairs (4%), mutations were present in both samples, but at allelic frequencies too low to support automated calling (<5%). Overall, this left a total of 39 sample pairs (15%) with definitive evidence of clonal evolution. Metastases were twice as likely to show novel mutations (23, 8.6%) as primary tumors (12, 4.5%). Novel mutations between primary and metastasis were found in 14 genes (AKT1, APC, CSF1R, CTNNB1, ERBB2, ERBB4, FBXW7, GNAS, KRAS, NRAS, PIK3CA, PTEN, PTPN11, SMAD4, TP53). TP53 was most frequently involved in clonal evolution (16 mutations), followed by PIK3CA (8 mutations), and SMAD4 (5 mutations).

Conclusions: Analysis of primary/metastasis by NGS showed concordance in the majority of samples. There was evidence of clonal evolution in 15% of tumors. Neoadjuvant therapy may lead to false negative results in primary tumor testing, highlighting the importance of optimizing preanalytic sample selection. Common secondary mutations involved tumor suppressor genes (TP53, SMAD4) as well as the potentially targetable oncogene PIK3CA.

1893 Novel Mutations in Therapy-Related and *De Novo* Myelodysplasia: Results from a Next-Generation Sequencing Pilot Study

RS Goswami, CY Ok, KP Patel, SA Wang, MJ Routbort, JH Manekia, KJ Jabbar, BA Barkoh, LJ Medeiros, RR Singh, R Luthra. UT MD Anderson Cancer Center, Houston, TX.

Background: 12 million cancer survivors in the US today have a 4.7 times higher risk of developing therapy-related myelodysplastic syndromes (t-MDS). High throughput platforms used in *de novo* MDS and targeted sequencing of t-MDS have shown somatic mutations that correlate with poorer disease outcome, however, no studies have concurrently compared t-MDS with *de novo* MDS using a common next-generation sequencing (NGS) platform. Here we describe a pilot study in which we used NGS to analyze 409 genes in both t-MDS and *de novo* MDS, to discern potential differences in the gene mutation profiles of these 2 entities.

Design: Five t-MDS and 5 *de novo* MDS patients were sequenced using the 409 gene Comprehensive Cancer Panel and the Ion Proton sequencer (Life Technologies). Each sample was sequenced to a minimum of 5 million AQ20 reads. Sequence alignment and variant calling was performed by TorrentSuite software v.3.6.2. Custom-built software (OncoSeek, UT MD Anderson), was used to examine variant calls and sequencing coverage, to filter sequencing artifacts and for annotation. A sequencing depth of 200X and 5% variant frequency were used as cutoffs for valid mutations.

Results: Average AQ20 reads and coverage depth per sample were 7.3 million at 380X. The total number of single nucleotide variants (SNVs) was similar between t-MDS and MDS (85 vs. 89) and included genes such as *FLT3*, *TET2* and *RUNX1*. Some of the identified SNVs were reported in the dbSNP database at low frequencies suggesting probable polymorphisms. The median number of SNVs was slightly higher in the t-MDS group compared with the *de novo* MDS group (16 vs. 12). Overall, SNVs were observed in 71 genes within the *de novo* MDS group compared with 59 genes within the t-MDS group. Of these genes, 23 were common to both groups. Frequently mutated genes (i.e. in 3 or more samples within a group) were seen more commonly within the t-MDS group and included *LRP1B* (4 of 5 samples) as well as *RNF213* (3 of 5 samples).

Figure 1. Venn diagram comparing genes common and unique to *de novo* MDS and t-MDS

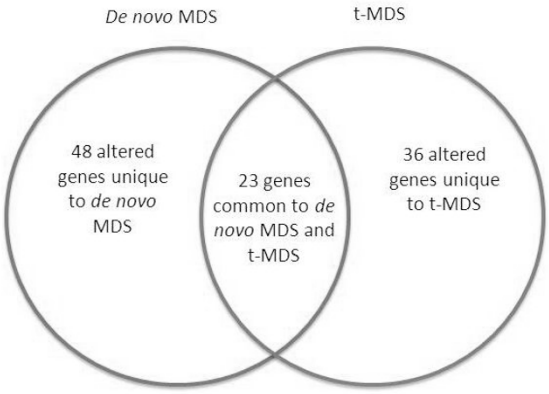

Conclusions: Using NGS methods we show numerous alterations unique to either t-MDS or *de novo* MDS. However, at least 23 genetic alterations were found to be common to both disease groups. Recurrent mutations were more frequently observed in t-MDS and involved *LRP1B* and *RNF213*.

1894 Understanding the Molecular Pathways Responsible for the Differences of Morphology and Differentiation between Common Appendiceal Tumors

X Gui, Z Meng, S Liu, Y McConnell, V Falck. University of Calgary, Calgary, AB, Canada.

Background: Classic carcinoid tumors (CCT), goblet cell carcinoid (GCC), low-grade mucinous neoplasm (LAMN) and mucinous carcinoma (MCA) are the most common tumors of appendix. They show different and sometimes mixed features. It was hypothesized that these diversified tumors may originate from a common tumor stem cell with potential of various lineage differentiation. In normal intestinal cell development, the commitment towards absorptive lineage (enterocyte) is driven by *Notch-Hes1* pathway, while the secretory lineage is driven by *Wnt-Math1(Hath1)* pathway but later separated by different downstream gene expression into three type of cells (*Gfi1-Klf4/Elf3* for goblet cell, *Gfi1-Sox9* for Paneth cell, and *Ngn3-Pdx1/Beta2/Pax4* for endocrine cell). We analyzed the expressions of these genes in different appendiceal tumor tissues to test the hypothesis.

Design: We have built a tissue microarray (TMA) of appendiceal tumors including GCC (133), LAMN (55), CCT (49), and MCA (33). The expressions of 9 genes (*Math1, Hes1, Gfi1, Ngn3, Sox9, Klf4, Elf3, Pax4,* and *TGF-βRII*) were detected by immunohistochemistry. The immunostain was semiquantitated as negative (0), 1+, 2+, and 3+. The expression of each gene product in different tumors was compared.

Results: In comparison with CCT, GCC showed a higher Klf4 expression but similar levels of Ngn3 and Pax4. The changes suggested that GCC showed a shift of cell differentiation towards goblet cells, but meanwhile kept a primary differentiation towards enteroendocrine cells. As compared to GCC, LAMN showed a higher expression of *Math1* ($p<0.001$), *Gfi1* ($p<0.001$), and *Klf4* ($p<0.001$), suggestive of an even stronger shift of differentiation towards secretory cell lineage, particularly goblet cells in LAMN than that in GCC. LAMN also showed a higher expressions of *Math1/Klf4/Ngn3/Pax4* and lower expression of *Hes1* as compared to MCA, suggestive of less differentiation towards enterocyte lineage but more towards secretory cell lineage in LAMN. However, contrary to what expected, GCC also showed a lower expression of *Ngn3* and *Pax4* than that in LAMN and a lower *Math1* and *Gfi1* expression than that in CCT.

Conclusions: Our data support that different gene expression patterns are related to the different morphologic features of different appendiceal tumors. The paradoxical lower *Ngn3* and *Pax4* in GCC as compared to LAMN and the lower *Math1* and *Gfi1* as compared to CCT may suggest a gain-of-function mutation of these four genes in GCC.

1895 mTORC2 Dependent Phosphorylation of Focal Adhesion Complex Proteins Critically Mediates Bladder-Cancer Cell Adhesion to Extracellular Matrices

S Gupta, W Zhou, J Harwalkar, TT Egelhoff, EF Petricoin, DE Hansel. Mayo Clinic, Rochester, MN; George Mason University, Manassas, VA; Cleveland Clinic Foundation, Cleveland, OH; University of California San Diego, La Jolla, CA.

Background: Cancer of the urinary bladder is ranked as the 5th leading cause of cancer worldwide and accounts for about 145,000 deaths annually. In an attempt to identify newer therapeutic avenues for these patients, our previous studies had shown that mammalian target of rapamycin complex 2 (mTORC2) dependent signaling frequently occurred in muscle-invasive UCas. In this study, we investigated the role of mTORC2 signaling in promoting an invasive phenotype.

Design: siRNA mediated mTORC2 ablation in malignant UCa derived J82 cells was used for downstream analysis. Functional assays included assessing attachment to various extracellular matrices, as well as to *ex vivo* cultures of bladder slices obtained from patients. Screening analysis, to identify novel mTORC2 phosphorylation targets was carried out by phosphopeptide enrichment followed by high-sensitivity nanospray liquid chromatography-coupled tandem mass spectrometry to identify regulators of cell adhesion. This was complemented with live cell imaging, where the novel target proteins were overexpressed, to better elucidate functional effects.

Results: mTORC2 ablation led to statistically significant reduction in cell adhesion to multiple extracellular matrices ($p<0.05$). Furthermore, these cells showed a significant reduction in attachment to the bladder slices ($p=0.002$). Novel phosphorylation targets of mTORC2 that were identified using the phosphoproteomic screening analysis were on the Serine 620 and 625 residues on the "KGLAGAVSELLRS" phospho-peptide, at the C terminus of Talin1. A complementary immunoblotting approach successfully identified mTORC2 dependent phosphorylation on Talin1, at an alternate functionally relevant phosphorylation site (Serine 425). Additionally, mislocalization of Talin1 was confirmed in mTORC2-ablated cells by live cell imaging.

Conclusions: Here, we report the identification of a novel target of mTORC2 regulation: Talin1, a key regulator of focal adhesion complexes. Our studies, therefore help delineate the specific mechanisms by which mTORC2 signaling promotes bladder cancer progression with implications for designing newer therapeutic agents.

1896 Mammalian Target of Rapamycin Complex 2 (mTORC2) Is a Critical Regulator of Bladder Cancer Invasion

S Gupta, JR Beach, J Harwalkar, E Mantuano, SL Gonias, TT Egelhoff, DE Hansel. Mayo Clinic, Rochester, MN; Cleveland Clinic Foundation, Cleveland, OH; University of California San Diego, La Jolla, CA.

Background: Bladder cancer accounts for greater than 70,000 new cancer cases annually and is the fourth most common cause of cancer in males, in the United States. Invasive behavior is a major determinant of prognosis. As mammalian target of rapamycin (mTOR) signaling has been identified as a regulator of disease progression, in this study, we evaluated the mTOR complex 2 (mTORC2) as a determinant of bladder cancer-cell migration and invasion.

Design: Benign papilloma derived RT4 cells and high-grade muscle-invasive UCa derived UMUC3, T24 and J82 cells served as an *in vitro* model system. Fresh tissue samples obtained from patients at the time of surgery were used for *ex vivo* bladder invasion assays and to determine signaling changes. mTORC2 function was interrogated by siRNA-mediated ablation of its unique constituent: Rictor, while its activity was assessed by the phosphorylation status of AKT-Ser473. Downstream changes in RhoA/Rac1 GTPase activation, Actin stress fiber formation and phosphorylation of the focal adhesion complex regulator: Paxillin was performed by a combination of immunoprecipitation, immunoblotting and immunofluorescence. Specific functional assessments included cell spreading, modified scratch wound migration, transwell invasion through a variety of extracellular matrices and a novel bladder slice invasion assay.

Results: Not only did the malignant cell lines demonstrate higher baseline mTORC2 activity relative to the benign papilloma-derived cell line, but also a 5-fold higher AKT-Ser473 phosphorylation was detected in specimens of invasive human bladder cancer as opposed to non-invasive disease. The malignant cells also demonstrated increased migration in transwell assays, invasion of Matrigel, and capacity to invade human bladder specimens. mTORC2 ablation substantially inhibited bladder cancer cell migration and invasion. This was accompanied by a significant decrease in Rac1 activation, decreased actin stress fiber formation and paxillin phosphorylation.

Conclusions: In this study, we identified mTORC2 signaling through Rac1 as a central regulator of bladder cancer cell migration and invasion. These studies suggest that selective mTORC2 targeting in invasive bladder cancer as a novel approach to patient therapy for neutralizing bladder cancer invasion.

1897 Comparison of Next Generation Sequencing Mutation Profiling with BRAF and IDH1 Mutation Specific Immunohistochemistry

KJ Jabbar, R Luthra, K Patel, R Singh, R Goswami, LJ Medeiros, K Aldape, MJ Routbort. UT MD Anderson Cancer Center, Houston, TX.

Background: Mutation-specific antibodies for BRAF V600E and IDH1 R132H offer convenient immunohistochemical assays (IHC) to screen for mutations in tumors. Previous studies have demonstrated high sensitivity and specificity in standardized test series, but use in routine qualitative clinical immunohistochemistry is less well studied. Next generation sequencing (NGS) mutation profiling assays offer an efficient means of assessing both known and novel oncogenic mutant proteins in tumor samples. Here we compared BRAF and IDH1 mutation specific IHC with NGS results.

Design: We retrospectively identified a total of 193 tumors where immunohistochemistry for BRAF V600E (VE1, Spring Bioscience) or IDH1 R132H (H09, Histobiotech) was performed using fixed, paraffin-embedded tissue sections, and subsequent NGS data from a 46-gene mutation panel (Ampliseq, Life Technologies) was also available. The IHC findings - classified as negative, positive, or equivocal - were compared with NGS data for concordance.

Results: For 67 tumors with combined IDH1 IHC and NGS data, IHC showed sensitivity of 98% and specificity of 100%.

IDH1 R132H

	NGS(-)	NGS(+)
IHC(-)	25	1
IHC(+)	0	41

Of note, 4 IHC-negative samples (6%) showed non-R132H IDH1 mutations (R132C x2, R132G, and P127T). For 128 tumors with combined BRAF IHC and NGS data, IHC showed sensitivity of 97% and specificity of 98% when including only cases with unequivocally positive or negative IHC results.

BRAF V600E (excluding equivocal IHC)

	NGS(-)	NGS(+)
IHC(-)	81	1
IHC(+)	2	31

However, a significant number of samples (13, 10%) had equivocal staining for BRAF V600E reported. Of these samples, 7 showed a V600E mutation by NGS. This finding significantly attenuated the sensitivity/specificity of V600E IHC depending on classification. If equivocal staining was considered a negative IHC result, sensitivity fell to 80%, while if equivocal staining was considered positive, specificity fell to 91%. Of note, 8 IHC-negative samples (6%) showed non-V600E BRAF mutations (N581I, V600K x5, V600M, K601E).

Conclusions: Our results suggest that the routine use of IHC for oncogenic proteins BRAF V600E and IDH1 R132H is relatively sensitive and specific, but has a non-trivial discordance rate. Equivocal interpretation for the BRAF V600E antibody stain significantly limited its predictive value. A significant percentage of cases had probable driver mutations that would be missed by IHC. These findings may limit the practical utility of routine mutation-specific immunohistochemistry as next-generation based sequencing of tumors becomes routine.

1898 Gene Amplification Patterns Identified by Next Generation Sequencing in a Large Tumor Cohort

KJ Jabbar, K Patel, A Ken, S Rajesh, B Russell, K Shaw, F Meric-Bernstam, RC Sinchita, L Alex, R Goswami, LJ Medeiros, L Rajalakshmi, M Routbort. UT MD Anderson Cancer Center, Houston, TX.

Background: Next generation sequencing (NGS) multigene assays have the potential to detect not only somatic mutations, but also abnormalities such as gene amplification. Since March 2012, we have tested over 4000 cancer samples using a mutation focused NGS panel (Ampliseq, Life Technologies). We report here a coverage-based analysis of this tumor population aimed at identifying recurrent genomic amplifications.

Design: An index of gene-level genomic representation (normalized coverage proportion [NCP]) was calculated for per gene as follows: [sum of average coverage depth for gene specific amplicons]/([sum of average coverage depth across all amplicons] x[number of gene specific amplicons]). This represents an internally normalized quantification of the coverage depth at a specific gene, with higher values indicating disproportionately elevated genomic representation. Previous validation data comparing NCP to clinical ERBB2 (Her2/neu) FISH results for this assay showed that samples with NCP(ERBB2)>0.02 all had clinically demonstrated ERBB2 amplification (positive predictive value 100%). We computed NCP values for 36 genes across 4196 DNA samples extracted from fixed, paraffin-embedded tumors.

Results: Reliability of the NCP metric was assessed by correlation analysis on a subset of patients who had had multiple NGS assays performed. Amplifications were highly concordant/correlated as shown below.

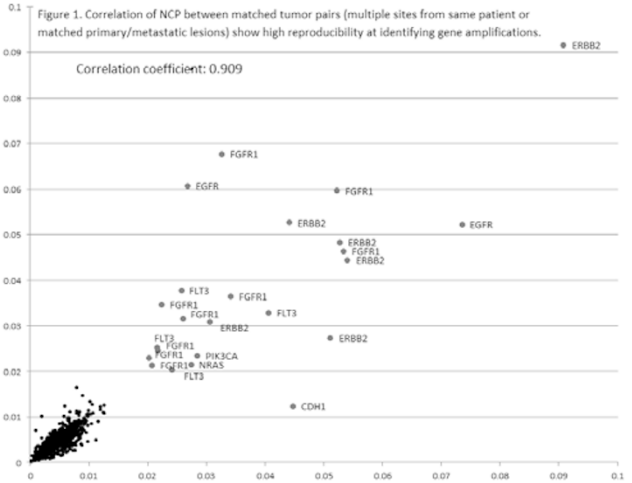

We identified a total of 331 gene-level amplifications across a set of 18 genes. 11 genes were recurrently amplified: EGFR,ERBB2,FGFR1,FLT3,KDR,KIT,KRAS,MET,NRAS,PDGFRA, and PIK3CA. Findings are summarized in figure 2.

Gene	Total	Breast	Colorectal	Glioma	Lung	Melanoma	Other
ALK	2	1					1
CDH1	2	1					1
EGFR	61	8	2	42	4		5
ERBB2	61	28	9		3	2	19
FGFR1	85	61	10		5	1	8
FGFR2	5	3	1				1
FGFR3	1					1	
FLT3	45		41				4
HNF1A	1				1		
KDR	16	1		4		9	2
KIT	12			4		8	
KRAS	6		1	1		2	2
MET	5	1			1	1	2
NRAS	11	4				5	2
PDGFRA	12	1		7		3	1
PIK3CA	4	3					1
PTPN11	1					1	
SMARCB1	1	1					

Conclusions: Distinct tumor specific amplifications were seen, with amplifications of ERBB2/FGFR1 in breast carcinoma, FLT3/FGFR1/ERBB2 in colorectal carcinoma, EGFR/PDGFRA in gliomas, and KIT/KDR/NRAS in melanoma. In addition, other tumor types showed sporadic amplifications of ERBB2, FGFR1, and EGFR, raising the possibility of targeted therapies for these neoplasms.

1899 Increased LGR5 Expression in Colonic Stem Cells Associated with Local Inflammation as an Early Events of Tumorigenesis

S Jain, Y Wu, E Richards, J Albanese, K Sun, EY Lin, Q Liu. Montefiore Medical Center, Bronx, NY.

Background: Chronic inflammation induced mutagenesis is likely to accumulate in the stem cells which have a long life span. However, the mechanism by which inflammation induces stem cell transformation is largely unknown. Cells distinguished by the expression of Lgr5 (Leucine-rich repeat-containing G-protein coupled receptor 5) have been implicated as colonic stem cells and are postulated to be important in colonic tumorigenesis.

Design: We have an established mouse model of colitis-associated colorectal cancer, Stat3-IKO, by inactivation of Stat3 specifically in macrophages. The mice spontaneously developed colitis and later form invasive adenocarcinoma. To study the effect of inflammation on colonic epithelial cells, Lgr5-GFP was crossed into Stat3-IKO. Immunostaining was performed using the primary antibody against LGR5 (Abgent) in 5 Stat3-IKO- Lgr5-GFP mice, and also in 16 randomly selected cases of human adenocarcinoma with their respective normal colonic tissue. The LGR5 staining was scored 0-3 based on the areas of highest intensity of the cell staining. The inflammation in the stroma was graded as low or high.

Results: Stat3-IKO-Lgr5-GFP mice with inflammation (n-=5), had expansion of Lgr5+ cells particularly at the base of the crypt as compared to normal. In inflammation with tumor mice (n=5), the tumors invasion fronts associated with chronic inflammation, also showed increased expression of LGR5. In human samples, the LGR5 reactivity was noted in few cells at the base of the crypts in normal colon similar to mice. There was also increase in number and intensity LGR5 positive cells in adenocarcinoma in comparison to their respective normal colonic tissue except in two cases. Out of 11 adenocarcinomas with LGR5 positivity score of 1; 5 had low grade (45%) and 6 had high-grade inflammation (55%). However all the cancers with LGR5 score of 2-3 had high grade inflammation (100%).

Conclusions: Our study shows a positive correlation of LGR5 expression with inflammation in the mouse model in colitis as well as in cancer at the invasive front. The study in human colon cancer also shows the positive correlation between LGR5+ cells and inflammation at the tumor invasion front. This study postulates a role of LGR5 pathway in colorectal adenocarcinoma tumor genesis especially in setting of chronic inflammation.

1900 Next Generation Sequencing in Soft Tissue Tumors: A Myth or a Reality?

G Jour, JD Scarborough, RL Jones, CC Pritchard, BL Hoch. University of Washington Medical Center, Seattle, WA; University of Washington School of Medicine, Seattle, WA.

Background: Next generation sequencing (NGS) is a novel molecular method providing in-depth detection of numerous gene alterations. To date, there are few published studies describing the use of this technique in soft tissue tumors. The aims of this study were to review our experience of NGS in a series of soft tissue tumors, and to test its utility in highlighting underlying molecular events as well as identifying targetable mutations.

Design: 15 cases were selected. NGS was performed using a clinically-validated multiplexed gene sequencing panel interrogating the full coding sequence of 194 cancer-related genes at 500X average coverage. A custom bioinformatics pipeline was developed to detect all classes of mutations directly from the NGS data, including single nucleotide variants (SNV), small insertions and deletions, copy number variation, and complex structural variation.

Results: Of the 15 patients 11 had metastatic and 4 localized primary disease.

Case	Age	Sex	Metastatic Site	Primary	Tumor type	FNCLCC grade
1	57	M	Left axilla *	Left scapula	Pleomorphic high grade spindle cell sarcoma with myofibroblastic differentiation	3
2	50	M	Mesentery *	Retroperitoneal	Leimyosarcoma	3
3	42	F	Spine T11 *	Retroperitoneal	Leimyosarcoma	2
4	37	F	Small bowel *	Uterus	Leimyosarcoma	2
5	51	M	NA	Stomach *	GIST	NA
6	65	F	NA	Stomach*	GIST	NA
7	64	F	Colon *	Small bowel	GIST	NA
8	59	F	Liver *	Liver	Angiosarcoma	3
9	36	F	Groin *	Leg	Angiosarcoma	3
10	42	F	NA	Atrial /inferior pulmonary vein mass *	Intimal sarcoma	2
11	45	M	Pelvic wall *	Knee mass	Clear cell sarcoma	3
12	35	M	NA	Foot *	Clear cell sarcoma	3
13	64	M	Lung *	Liver	Epithelioid Hemangioendothelioma	NA
14	48	F	Lung *	Thigh	Pleomorphic spindle cell sarcoma	3
15	35	M	Small bowel *	Uterus	Sclerosing epithelioid fibrosarcoma	NA

*Refers to the specimen that was subjected to Next Generation Sequencing.

Targetable mutations for which clinical trials are available were identified in 60% of the cases. Copy losses of the *TP53, PTEN* and *CDKN2A* genes were frequently recurring molecular events in our series. Additional non-targetable novel variants including copy losses, frameshift mutations and SNVs were also identified.

Case	Targetable/Actionable mutations	Clinical Impact / Available Trial number (www.clinicaltrial.gov)	Additional identified variants
1	Copy gain in *MYCL1* (LMYC)	Phase I Study Of Aurora Kinase Inhibitor PF-03814735 In Patients With Advanced Solid Tumors / (NCT00858403)	Homozygous loss of *TP53* and *RB1* genes SNV involving *PIK3R1*, *PDGFRB*, *BRAF48*, *KDM6A* and *FLT3*
2	FGFR1 amplification Copy gain of *MYC*	Dose Escalation Study of Oral BGJ398, a Pan FGF-R Kinase Inhibitor, in Adult Patients With Advanced Solid Malignancies / (NCT01004224) A Phase I, Dose-finding Study of the Aminobenzimidazole (BnB) Inhibitor OTX015 in Hematological malignancies(NCT01713802)	Homozygous loss of *PTEN* SNV involving *IGF1R* (p.G1225S)
3	*MAP2K4* Amplification Copy gain in chromosome 8 (in a region including *FGFR1*) Copy gain of *MYC*	Phase I Study of WX-837 Alone and in Combination With WX-554 in Solid tumors (NCT01858051) Dose Escalation Study of Oral BGJ398, a Pan FGF-R Kinase Inhibitor, in Adult Patients With Advanced Solid Malignancies (NCT01004224)	*PTEN* copy loss and frame shift mutation *NF1* copy loss and frame shift mutation Copy losses of *MPI*, *TP53*, and a portion of *RMS2*
4	*MAP2K4* Amplification Copy gain in chromosome 8 (in a region including *FGFR1*) Copy gain of *MYC*	Phase I Study of WX-837 Alone and in Combination With WX-554 in Solid tumors (NCT01858051) Dose Escalation Study of Oral BGJ398, a Pan FGF-R Kinase Inhibitor, in Adult Patients With Advanced Solid Malignancies / (NCT01004224)	Copy losses in portions of chromosomes 10 Copy losses in portions of chromosomes 17 (including *RAI1* and *TP53* genes) Copy losses in chromosome 6 (in a region including *PTEN*)
5	KIT exon 11 deletion mutation (p.V559A)	GIST with deletions in exon 11 has been reported to be generally sensitive to imatinib (Lasota 2000, Medinger 2013).	SNV involving *PLT4* (p.S174L)
6	KIT exon 11 point mutation (p.V559A)	GIST with (p.V559A) mutations has been reported to be sensitive to imatinib therapy (Lasota 2000, Medinger 2013).	frameshift mutation in *ERBB4* gene Copy losses of *CDKN2A* and *KIT* genes
7	KIT exon 11 in-frame duplication mutation (p.Pro573_His580) / KIT exon 13 resistance mutation (p.V654A) FGFR1 copy gain	KIT (p.V654A) confers resistance to imatinib and causes drug resistant relapse in GIST patients (Roberts 2007). Dose Escalation Study of Oral BGJ398, a Pan FGF-R Kinase Inhibitor, in Adult Patients With Advanced Solid Malignancies / (NCT01004224)	Homozygous loss of the *CDKN2A* gene SNV involving *MOTOR* (p.V215L) and *PIK3R1* (p.R391G) genes
8	None	NA	48bp deletion mutation in exon 1 of *NPR4* gene. 1 bp deletion in exon 1 of *NYP4* gene resulting in a premature frame shift and loss of function (NM_80424084.1:c.44del, p.Leu15*) Copy gain in chromosome 21 (in a region including *RUNX1* gene
9	CDK4 and MDM2 gene amplification Copy gains of chromosomes 4 (in a region including *FGFR3*) and 8 (in a region including *FGFR1*)	A Study of PI3K/MTOR Inhibitor With Doxorubicin in Patients With Soft Tissue Sarcoma / (NCT01658826) Dose Escalation Study of Oral BGJ398, a Pan FGF-R Kinase Inhibitor, in Adult Patients With Advanced Solid Malignancies / (NCT01004224)	Copy losses in *CDKN2A* gene. Copy losses in portions of chromosome13 (in a region including *FOXO1*) Copy losses in chromosome16 (in the region of *CDH1*)
10	FGFR1 and *MYC* copy gain	Dose Escalation Study of Oral BGJ398, a Pan FGF-R Kinase Inhibitor, in Adult Patients With Advanced Solid Malignancies (NCT01004224)	Copy losses in chromosomes 3 (includes *RASSF1*), 9 (includes *CDKN2A*), and 17 (in a region including *TP53*)

Note: Cases 8, 11, 12, 14, and 15 are not included (no mutations identified)

Conclusions: Our study suggests that NGS has utility in identifying targetable mutations in soft tissue tumors. This could serve as a rationale for selecting patients with advanced disease for clinical trials. Furthermore, a number of variants that may be involved in the pathogenesis of these tumors were also identified. The limitations include cost and non-standardized interpretation method. Further prospective studies with larger numbers are needed to validate our findings.

1901 Expression of Cancer Testis (CT) Antigen NY-ESO-1 in Non-Small-Cell-Lung Cancer and Correlation with Serology

AA Jungbluth, N Altorki, D Frosina, E Ritter, CF Spinelli, S Gnjatic. Memorial Sloan-Kettering Cancer Center, New York, NY; New York Presbyterian Hospital, New York, NY; Mount Sinai Hospital, New York, NY.

Background: CT antigens are expressed in various types of cancers but silent in most normal tissues except testicular germ cells. CT antigens have been identified by their ability to elicit autologous immune responses in cancer patients and NY-ESO-1

is among the most immunogenic CT antigens triggering serological and/or cellular immune responses in various cancer types. Due to their tumor-associated expression and their immunogenicity, CT antigens, in particular NY-ESO-1, have been used as vaccine target in various clinical immunotherapy trials. Interestingly, little is known about the association of the actual NY-ESO-1 protein expression in tumors and the autologous serological immune response in cancer patients. Consequently, we analyzed the NY-ESO-1 protein expression as well as serum titers to NY-ESO-1 in a large cohort of patients with NSCLC.

Design: Matched tissue and serum samples were collected from 194 lung cancer patients at time of surgical primary resection. Expression of NY-ESO-1 was analyzed by standard IHC techniques employing mAb E978 previously generated by our group. Serum was collected at the time of surgery and NY-ESO-1 serum titers were analyzed by ELISA using full-length NY-ESO-1 protein. Several grading systems for the IHC staining were tested.

Results: NY-ESO-1 was present in 33/194 (17%) lung tumors. NY-ESO-1 expression was graded based on the amount of immunopositive cells as follows: focal (<5%) 8/33, + (5-25%) 10/33, ++ (25-50%) 5/33, +++ (50-75%), 1/33, and ++++ (>75%) 9/33. The cut-off for significance of NY-ESO-1 serum titers was 1:100 and 17/194 were positive: 3 weak (titers 1:100-1:1000), 6 moderate positive (1:1000-1:10000), 8 (strong positive (>1:10000). 14/17 (82%) sero-positive sera were present in patients with corresponding NY-ESO-1 protein expression in the tumor. Interestingly, positive serum titers were mostly (10/17) found in patients with NY-ESO-1 expression in at least 25% of the tumor. Only 2 patients with positive serum titers showed focal NY-ESO-1 expression and three were completely negative.

Conclusions: Positive serological immune responses to NY-ESO-1 in NSCLC are mostly present to patients with extensive NY-ESO-1 expression in the primary tumor. NY-ESO-1 serum titer levels appear to correspond to the extent of protein expression in the tumor. The relation of protein expression to serum titers has important implications for future monitoring of clinical trials employing CT antigens.

1902 Aggressive/Metastatic Prostatic Adenocarcinoma Cancer (PAC): Molecular Characterization by miRNA Expression Profiling May Explain Aggressive Behavior

R Kolhe, P Vasa, S Kavuri, J Lee, A Rahardja, A Rojiani, V Kota. Georgia Regents Univeristy, Augusta, GA; Georgia Regents University, Augusta, GA.

Background: Current prognostic markers of high grade/aggressive/metastatic tumors after radical prostatectomy are limited, and therapy with androgen-deprivation leads to important side effects. To better understand the molecular mechanisms of this aggressive PAC we analyzed 29 PAC resection specimens (N0=20 & Nx=9).Recently, a class of noncoding RNAs called miRNAs has emerged as critical gene regulators in cell growth, disease, and development. The goal of the current study was to evaluate the similarities and differences in localized and metastatic PAC at mirna level.

Design: Archival blocks with slides were retrieved, reviewed and clinical information obtained from patient charts. Ten 10µm sections of each case were used with >50% lesion. Based on the published PAC onco-miRNAome a 38 miRNA panel was designed. Along with the onco-miRNA's it included 4 house keeper, 2 scrambled, and 2 normalizing miRNA. The Array Plate is then imaged via HTG's Super Capella to measure the expression of every gene in all of the wells. Samples were run in triplicate and data was normalized to RPL19 expression.

Results: The array showed a statically significant clinically relevant set of tumor suppressor miRNA's (mir-let7c, mir-26a and mir-145) was decreased and mir-21 expression was increased in metastatic PAC vs localized PAC.

Conclusions: We know by target prediction methods that 3' untranslated region of the ERG mRNA is a potential target of miR-145 and recent studies show that down-regulation of miR-145 may contribute to the increased expression of most ERG splice variants and hence aggressive disease. Also, let-7c is well documented tumor suppressor microrna located on 21q21 which shows frequent loss in metastatic tumors. Loss or reduction of let-7c also leads to Ras overexpression, thus, promoting cellular growth and contributing to tumor genesis. In contrast, miR-21, located on chromosome 17q23.1, is the most commonly overexpressed oncogenic miRNA & is associated with a poorer prognosis in most of the tumors. In this study, we found a significant correlation between the over-expression of miR-21and higher Gleason scores. We propose that this down regulation of the tumor suppressor miRNA's and mir-21 overexpression in metastatic PCA may explain some of the very aggressive behavior. This work is intriguing for the new information it provides about the complete set of deregulated mirna's in aggressive patients.

1903 Role of Intracellular Calcium and NADPH Oxidase NOX5-S in Acid-Induced DNA Damage in Barrett's Esophageal Adenocarcinoma Cells

D Li, W Cao. The Warren Alpert Medical School of Brown University & Rhode Island Hospital, Providence, RI.

Background: Gastro-esophageal reflux disease complicated by Barrett's esophagus (BE) is a major risk factor for esophageal adenocarcinoma (EA). The mechanisms whereby acid reflux may accelerate the progression from BE to EA are not fully understood. Acid and reactive oxygen species (ROS) have been reported to cause DNA damage in Barrett's cells. We have previously shown that NADPH oxidase NOX5-S is responsible for acid-induced H_2O_2 production in Barrett's cells and in EA cells. In this study we examined the role of intracellular calcium and NADPH oxidase NOX5-S in acid-induced DNA damage in a Barrett's EA cell line FLO.

Design: DNA damage was measured by using a Comet assay which is based on the ability of denatured cleaved DNA fragments to migrate out of the cell under the influence of an electric potential. It is quantitated by measuring the tail length, tail area and tail moment. The phosphorylation of histone H2AX was examined by Western blot analysis. Intracellular calcium was measured in Fura-2AM loaded cells.

Results: We found that pulsed acid treatment significantly increased tail length, tail area, tail moment and histone H2AX phosphorylation in FLO cells. In addition, acid treatment significantly increased intracellular Ca^{2+}, an increase which is blocked by Ca^{2+} free medium with EGTA and thapsigargin. Acid-induced increase in tail length, tail area, tail moment and histone H2AX phosphorylation was significantly decreased by blockade of intracellular Ca^{2+} increase, by NADPH oxidase inhibitor diphenylene iodonium and by knockdown of NOX5-S with NOX5 siRNA. Conversely, overexpression of NOX5-S significantly increased tail length, tail area, tail moment and histone H2AX phosphorylation.

Conclusions: Pulsed acid treatment causes DNA damage via increase of intracellular calcium and activation of NOX5-S. It is possible that in Barrett's esophagus acid reflux increases intracellular calcium, activates NOX5-S and increases ROS production, which causes DNA damage, thereby contributing to the progression from BE to EA.

Supported by NIH NIDDK R01 DK080703.

1904 Targeted Identification of Potential Protein Biomarkers in Bronchoalveolar Lavage (BAL) Fluid from Lung Cancer Patients

QK Li, WM Yang, MH Ao, E Gabrielson, F Askin, DW Chan, H Zhang. The Johns Hopkins Medical Institutions, Baltimore, MD.

Background: Currently, bronchoalveolar lavage (BAL) is commonly used for the cytological evaluation of lung nodules and diagnosis of lung cancers, but proteins in the BAL fluid are not examined in clinical practice, might also serve as potential biomarkers for cancer diagnosis. Recent clinical screening trials using highly sensitive low-dose computed tomography (LDCT) demonstrated an improved overall survival of lung cancer patients as the result of early detection of stage I lung cancers. However, these lung cancer screening trials also showed high repeat screening rates and false-positive rates causing unnecessary second-line invasive procedures and surgery. New strategies are needed to improve the specificity of lung cancer screening. In this study, we investigated the protein profile in BAL fluid and their potential utility as biomarkers in diagnosing lung cancer.

Design: BAL fluids were collected after cellular components were harvested for cytological examination in the cytology laboratory. Protein profiles, with a focus on *N*-glycoproteins, were analyzed using the solid-phase extraction of *N*-glycoprotein (SPEG) and liquid chromatography tandem mass spectrometry (LC-MS/MS). Sixteen BAL samples, including four cases each of benign lung disease, adenocarcinoma (ADC), squamous cell carcinoma (SqCC), and small cell carcinoma (SCLC), were evaluated for this study. The levels of glycoproteins in BAL were further assessed by ELISA assays using independently collected 75 BAL specimens.

Results: A total of 1081 unique peptides from 468 glycoproteins were identified and quatified in cancer and benign BALs. Among them, levels of 133 glycoproteins were significantly altered in cancer BALs than that of benign BALs ($P<0.05$), including 43 glycoproteins in ADCs, 56 in SqCCs, 34 in SCLCs. The utility of several glycoproteins such as galactin3 binding protein, myeloperoxidase and a few others in the diagnosis of lung cancers were further evaluated using independently collected BAL specimens by ELISA assays. The sensitivity and specificity of these glycoproteins were varied and ranged from 33.3% to 83.3%, and 42.6% to 100%, respectively.

Conclusions: Our study demonstrates that potential protein biomarkers in BAL fluid can be quantified. They have the potential to improve the specificity of lung screening tests and to reduce unnecessary surgery in patients with benign lung nodules. A large scale of study is needed to further validate our findings.

1905 LCM-NGS: Tumor Cell Enrichment by Laser Capture Microdissection (LCM) Significantly Improves Next-Generation Sequencing (NGS) of Pancreatic Cancer Whole Genomes

S-B Liang, N Buchner, M Sam, JD McPherson, MHA Roehrl. University Health Network, Toronto, ON, Canada; Ontario Institute for Cancer Research, Toronto, ON, Canada.

Background: Next-generation sequencing (NGS) provides a powerful platform for deep insight into the precise genetic make-up of cancers. However, real-life application of NGS to primary patient tumors is often severely limited by scarcity of tumor cells in tissue and by heterogeneity of the non-neoplastic compartment (fibrosis, entrapped benign cells, etc.). Laser capture microdissection (LCM), an efficient tool for precisely collecting target cells, may substantially improve NGS quality.

Design: As part of the International Cancer Genome Consortium, we collected fresh frozen pancreatic ductal adenocarcinomas. We used LCM for tumor cell enrichment on 26 patients. Non-microdissected tumors and benign tissues were also collected. DNA was extracted and NGS libraries were constructed for each sample. NGS was carried out on Illumina HiSeq 2500 instruments. We used deep quantitative NGS allele read counts of the KRAS gene (mutated in >90% of pancreatic cancers) to assess the completeness of tumor cell enrichment provided by LCM over non-enriched primary tumors.

Results: DNA has been extracted from all 26 cases, with a median DNA yield of 150 ng per 100,000 cells collected. Careful LCM of one cancer case takes approximately one working day and involves isolation of 200,000-600,000 tumor cells. Whole cancer genome sequencing of seven cases has been completed. KRAS mutant allele frequencies of non-LCM primary tumor samples ranged from 9-19% (indicating 18-38% tumor cell content). KRAS mutant allele read counts after LCM enrichment showed values from 20-50% (indicating 40-100% tumor cell purity). Based on deep NGS KRAS mutant allele frequencies of LCM and non-LCM samples, tumor purity enrichment was 4.0-4.4-fold in four cases and 3.0-fold, 2.6-fold, and 1.1-fold in the other three cases. Somatic copy number alteration analyses also show much cleaner data across the genome over non-LCM samples. Whole genome assembly and comprehensive mutation calls are underway for all cases.

Conclusions: Our analysis demonstrates the tremendous utility of LCM for successfully enriching tumor content from low-cellularity cancer samples to near-complete purity resulting in dramatically superior whole genome sequence data and thus making

downstream bioinformatics analyses easier. We established a routine LCM-NGS workflow pipeline that will be widely applicable to deep sequencing of any primary human tumor.

1906 Analysis of Epithelial Neoplasms of the Appendix Using the Ampliseq Cancer Hotspot Mutation Panel

X Liu, K Mody, JM Pipas, KD Smith, JD Peterson, F de Abreu, TL Gallagher, CI Amos, AA Suriawinata, GJ Tsongalis. Geisel School of Medicine at Dartmouth, Hanover, NH and Dartmouth Hitchcock Medical Center, Lebanon, NH.

Background: Some of the epithelial neoplasms of the appendix, including low-grade appendiceal mucinous neoplasm and adenocarcinoma can result in the clinical picture of pseudomyxoma peritonei (PMP). Little is known about the mutation spectra in these tumor types and whether mutations may be of clinical significance with respect to potential therapeutic selection. In this study, we identified somatic mutations in a 50 gene panel (Ion Torrent AmpliSeq Cancer Hotspot Panel v2) using next-generation sequencing (NGS).

Design: Specimens consisted of 1 non-neoplastic mucocele, 7 low-grade mucinous neoplasms, 5 well differentiated mucinous adenocarcinomas with PMP, and 5 appendiceal cancers including 2 goblet cell carcinoid-adenocarcinomas and 3 signet ring cell carcinomas. Each specimen was reviewed by a pathologist for percent tumor cell content and DNA was extracted from 8 unstained four micron sections. Barcoded libraries were prepared from up to 10ng of extracted DNA and multiplexed on single 318 chips. Data analysis was performed using Golden Helix SVS. Variants that remained after the analysis pipeline were individually interrogated using the Integrative Genomics Viewer (IGV).

Results: A single JAK3 mutation was detected in the mucocele while 5/7 low grade neoplasms had KRAS and GNAS mutations. Additional mutations in the low grade cases included APC (4/7), RB1 (2/7), JAK3 (1/7), STK11 (1/7), PIK3CA (1/7), and MET (1/7). The mutation spectrum of the five PMPs included KRAS (4/5), GNAS (1/5), TP53 (2/5) and RB1 (1/5). KRAS, TP53, IDH1 and ATM mutations were each found in one of the five appendiceal cancer cases. In addition, three of these cases had SMAD4 mutations.

Conclusions: Our results suggest molecular heterogeneity among epithelial tumors of the appendix. NGS efforts have identified mutation spectra in several subtypes of these tumors that may suggest a phenotypic heterogeneity that warrants further study.

1907 Genetic Alterations in Small Intestinal Versus Appendiceal Neuroendocrine Tumors Detected by Whole Exome Next Generation Sequencing

S Lu, L Dong, V Breese, C Jackson, A Snow, M Resnick, E Yakirevich. Alpert Medical School of Brown University, Providence, RI; Brown University, Providence, RI.

Background: Gastrointestinal neuroendocrine tumors (NETs) comprise a heterogenous group of neoplasms with a varying spectrum of aggressiveness. Small intestinal NETs (SI-NETs) are biologically aggressive tumors with a greater metastatic potential than appendiceal NETs (A-NETs). Known genes that are frequently mutated in other cancers, such as *TP53*, *K-RAS*, *BRAF*, and *PIK3CA* are only rarely present in NETs. In this study we characterized the genomic profile of SI-NETs and compared the genetic alterations between SI-NETs and A-NETs by whole exome next generation sequencing (WES).

Design: We analyzed 3 primary SI- NETs, 2 A-NETs and matched normal tissues. Genomic DNA was isolated from the tumor cells after laser capture microdissection (Arcturus) from FFPE sections. Genomic DNA libraries were constructed, exomes captured with the Agilent SureSelect XT kit, and sequenced on the Illumina HiSeq 2000 system. Bioinformatics were applied to analyze somatic single nucleotide variants (SNVs).

Results: Whole exome sequencing had an average depth of 26 reads and identified 2,335 SNVs throughout all 5 NETs. Our bioinformatics filtering approach narrowed down the number of somatic mutations by removing germline variants identified in the matched normal tissues, and variants from 1,000 genomes and dbSNP dabases while keeping variants catalogued in the Catalog of Somatic Mutations in Cancer (COSMIC). As a result, 68, 88, and 89 nonsynonymous SNVs were identified in 3 SI-NETs, while in A-NETs the number of SNVs was lower (48 and 42). We then focused on genes mutated in at least 2 tumors. *AK2* was mutated in all 3 SI-NETs but not in any A-NETs. *MAP2K3*, *PLIN4*, *IYD*, *SVIL*, and *KCNJ* were mutated in 2 SI-NETs but not in any A-NETs. In addition, Ingenuity Pathway Analysis (IPA) identified mutations involved in the ERK pathway, including the metastasis suppressor gene *KISS-1*. Mutations in selected genes of interest, including *KISS-1*, *MAP2K3*, and *PDE4DIP* were confirmed by Sanger sequencing.

Conclusions: This is the first study to compare genetic alterations between small intestinal and appendiceal NETs. Although the overall mutation rate in NETs is low, SI-NETs are characterized by a higher frequency of somatic SNVs as compared to A-NETs. Mutations in the metastasis suppressor gene *KISS-1* may play a role in the pathogenesis of these tumors and may be a potential target for treatment of this aggressive neoplasm.

1908 The Genomic Landscape of Adenoid Cystic Carcinoma of the Breast

LG Martelotto, CK Ng, R Lim, S Piscuoglio, R Natrajan, D Wetterskog, P-E Colombo, JS Reis-Filho, A Vincent-Salomon, B Weigelt. Memorial Sloan-Kettering Cancer Center, New York, NY; Institute of Cancer Research, London, United Kingdom; CRLC Val d'Aurelle, Montpellier, France; Institut Curie, Paris, France.

Background: Adenoid cystic carcinoma (AdCC) is a malignant neoplasm most commonly diagnosed in the salivary glands, but also found in other gland-rich tissues such as the breast, lung and prostate. AdCC of the breast is a rare (<1%) special histological type of breast cancer that is usually of triple-negative phenotype and has an indolent clinical behavior. The defining molecular feature of both salivary gland and breast AdCCs is the activation of *MYB*, which is usually caused by a recurrent translocation t(6;9) that results in the formation of the *MYB-NFIB* fusion gene. We have previously demonstrated that breast AdCCs display patterns of gene copy number aberrations distinct from those of other triple-negative breast cancers. In this study, we sought to define the mutational landscape of breast AdCCs.

Design: DNA was extracted from 6 microdissected pure AdCCs of the breast and subjected to whole exome sequencing. Alignment was performed using bwa. Single nucleotide variants were detected by MuTect and MutationSeq, and insertions and deletion (indels) were determined using GATK. Bioinformatic algorithms (CHASM, FATHMM and Mutation Assessor) were employed to distinguish driver from passenger mutations.

Results: We confirmed the presence of the *MYB-NFIB* fusion in all cases. Similar to salivary gland AdCCs, we found that breast AdCCs had low mutation rates (4-13 non-silent events per tumor). No recurrent mutations were identified; however, we observed that pathways and cellular functions including chromatin regulation, transcription factors, RNA metabolism, signaling pathways, cell adhesion, and DNA repair were recurrently targeted by potentially pathogenic mutations. Furthermore, alterations were identified in known cancer genes, including, *BRAF, MYB, PRKD1* and *GRIN2A*, in addition to driver mutations in *RASA1, PTPN7,* and *CYLD*, a gene whose mutations result in familial cylindromatosis. Finally, one case harbored a *SF3B1* hotspot mutation at codon R625, which has recently been reported in uveal melanoma, chronic lymphocytic leukemia, and salivary gland AdCCs, and is associated with differential alternative splicing.

Conclusions: Our results demonstrate that AdCCs of the breast do not harbor *TP53* mutations like other triple negative breast cancers, but are similar to AdCCs of the salivary gland in terms of mutational burden, pathways recurrently affected by mutations and genome stability.

1909 Phosphorylation of eIF4E Associates with Lymph Node Metastases in Breast Carcinomas and Confer Resistance to Cellular Stress and Treatment with DNA-Damaging Agents

A Martinez, T Aasen, M Sese, B Castellana, I Sansano, V Peg, S Ramon y Cajal. Molecular Pathology, Vall d'Hebron Research Institute, Autonomous University of Barcelona, Barcelona, Spain; Vall d'Hebron University Hospital, Barcelona, Spain.

Background: Malignant cells develop resistance to hypoxia, starvation, oxidative stress and various therapeutic treatment modalities by poorly defined mechanisms. Because phosphorylation of eIF4E is associated with transformation and prognosis in human tumors, we analyzed the expression of phospho-eIF4E in breast carcinomas and the role of phospho-eIF4E in resistance to cellular stress and DNA-damaging agents in vitro.

Design: Eighty breast carcinomas were analyzed by immunohistochemistry and western blot for the expression of pMAPK, mTor, 4E-BP1, p4E-BP1, eIF4E, phospho-eIF4E, and EMT factors (N-cadherin, snail, slug, vimentin,). Breast carcinoma cell lines (MDA-MB 231, MBA- MB 468), HeLa cells and HaCaT keratinocytes were infected with retrovirus to express wild type, phospho-mimetic (S209D) or phospho-dead (S209A) mutants of eIF4E. Cells were subjected to stress including oxidative (Arsenite), nutrient starving (glucose) and cisplatin treatment, and were subsequently evaluated using colony formation assays, MTT cell proliferation assays as well as co-immunoprecipitation and western blot analysis of proteins related to apoptosis and proliferation.

Results: In the clinical series, primary breast tumour with lymph node metastases showed elevated expression of phospho-eIF4E compared with lymph node negative tumors (p: 0,041). Moreover, peIF4E associated with high Ki67 positivity and higher expression of the epithelial mesenchymal factor slug. In vitro, cell lines expressing the phophomimetic form of eIF4E were more resistant to DNA-damaging agents (such as cisplatin), glucose starvation and oxidative stress (arsenite). Fibroblasts derived from Mnk1/2 knock-out mice and breast carcinoma cell lines treated with the Mnk1/2 kinase inhibitor CGP57380, which prevent phosphorylation of eIF4E, were significantly more sensitive to cisplatin and arsenite.

Conclusions: With these data, we demonstrate that high levels of phospho-eIF4E associates with lymph node metastases in breast carcinomas. Phosphorylation of eIF4E confers resistance to cellular stress. Treatment with inhibitors of eIF4E phosphorylation increases the sensitivity to treatment with DNA-damaging agents, supporting the rationale for combining these inhibitors with cytotoxic drugs for the treatment of breast carcinomas.

1910 Large Scale Phophoproteomic Analysis Reveals That Wiskott-Aldrich Syndrome Protein Regulates the Clonogenic Potential of Anaplastic Large Cell Lymphoma Via Modification of Survival Signaling Pathways

C Murga-Zamalloa, V Mendoza-Reinoso, V Basrur, K Elenitoba-Johnson, MS Lim. University of Michigan, Ann Arbor, MI.

Background: Mutations in the Wiskott-Aldrich syndrome protein (WASp) are associated with immunodeficiency. Patients with mutations in WASp often develop lymphoma, however the mechanism is not completely understood. Anaplastic large cell lymphoma (ALCL) is a subtype of mature T cell lymphoma and is the most common type of T cell lymphoma in the pediatric population. Most cases are associated with the chromosomal translocation t(2;5)(p23;q35) resulting in the expression of NPM-ALK which is a constitutively active oncogenic tyrosine kinase. Recently, we demonstrated that phosphorylation of WASp by NPM-ALK at a novel site, Y102 contributes to the oncogenicity of ALCL. In order to better understand the role of WASp in oncogenesis, we utilized an unbiased mass spectrometry –based phosphoproteomic approach to identify downstream signaling pathways regulated by WASp phosphorylation.

Design: ALCL-derived cell lines stably expressing GFP tagged WT, Y102F WASp or GFP alone were generated with lentiviral-mediated transduction. The phosphoproteome was enriched using a two-step procedure including immobilized metal affinity

chromatography (IMAC) and phospho-tyrosine immunoaffinity purification and subsequently analyzed by liquid chromatography and high mass accuracy tandem mass spectrometry (LC-MS/MS). Statistical significance of phosphorylation changes was calculated with qSpec online software.
Results: The phosphoproteomic analysis identified 16 proteins involved in actin dynamics (including CRKL and ARP2/3 complex) to be modified after overexpression WASp. Subsequent analysis with NCI pathway database revealed that the majority of these proteins participate in a network that modulates actin polymerization through cdc42 activation. The other major group of proteins regulated by WASp overexpression represents those involved in apoptosis and cell cycle progression. Signaling pathway analysis showed that these proteins are members of MAPK, SHP2. Interestingly, the majority of these proteins were differentially phosphorylated between WT and Y102F WASp.
Conclusions: Our data suggest that phosphorylation of WASp at Y102 modifies signaling pathways involved in apoptosis and cell cycle progression. These results are in accordance with the hypothesis that phosphorylation of WASp at Y102 increases the clonogenic potential for ALCL. Our results show for the first time that WASp has a direct role in oncogenesis via regulation of cell cycle progression and apoptosis signaling.

1911 Incorporation of PTEN Status Determination in Routine Molecular Prescreening for Targeted Therapies

P Nuciforo, L Prudkin, C Aura, J Jimenez, N Peiro, P Martinez, A Vivancos, D Moreno, J Rodon. Vall d'Hebron Institute of Oncology, Barcelona, Spain.
Background: Enriching PhI trials with patients harboring alteration in the Pi3K pathway is key to the successful development of PI3K pathway inhibitors. Beside PIK3CA mutations, PTEN loss as determined by immunohistochemistry (IHC) is being considered an indicator of Pi3K pathway alteration.
Design: An ISO-accredited PTEN IHC assay was run in tumor samples from candidates to enter a PhI clinical study. PTEN status was defined as loss when tumor H-score < 50 (0-300). Mutations in key oncogenes were assessed using multiplexed MassARRAY platform (Sequenom) on DNA obtained from the same block used for IHC.
Results: From Jan 2012 we received 737 PTEN requests. Evaluable sample population (ESP) was 685 samples (93%). Samples came from primary tumors in 520 cases (PT=70%) and metastatic disease in 168 cases (MET=23%). In 49 cases (7%) the sample origin was unknown (UKN). Among ESP, PTEN loss was observed in 33% of cases, with a loss rate similar for PT (n=160, 33%), MET (n=48, 31%) and UKN (n=17, 37%). After subgrouping by tumor origin, 42% (n=71), 21% (n=11), and 18% (n=17) of PT from colorectal cancer (CRC), ovarian cancer (OC), and breast cancer (BC) showed loss of PTEN, respectively. PTEN loss rates observed in MET from the same tumor types were 42% (n=17), 44% (n=4), and 24% (n=7) respectively for CRC, OC, and BC. A total of 211 mutations across 10 genes (AKT1, BRAF, EGFR, FGFR3, GNAQ, IDH1, KRAS, NRAS, PDGFRA, PIK3CA) were observed in 183 (38%) of 476 samples with available PTEN IHC data. KRAS was the most frequent mutation (n=104, 49%) followed by PIK3CA (n=65, 31%) and BRAF (n=19, 9%). Overall, PTEN loss rate was similar in tumor with (n=69, 38%) and without mutations (n=89, 30%). PTEN loss was less frequent in PIK3CA mutant (17%, n=11/65) compared to PIK3CA WT (36%, n=147/411) (all tumor types, p=0.003). This inverse correlation remained significant in CRC but not in BC after stratifying by tumor type. Conversely, PTEN loss was higher in KRAS (45%, n=47/104) mutants compared to WT (30%, n=111/372) (all tumor types, p=0.003). Correlation between KRAS mutations and PTEN loss was not significant when analyzing CRC only.
Conclusions: These large consecutive analysis of PTEN show that its incorporation in a routine molecular prescreening is feasible. From our results it can be infer that PTEN loss is similar between primary and metastatic sites and that may vary according to tumor genetic background and organ of origin. These data may provide clinicians with a tool to better select patients to targeted therapies.

1912 MED12 Is a Potential Target for Therapeutic Intervention in Castration Resistant Prostate Cancer

A Offermann, Z Shaikhibraim, M Braun, R Menon, D Bohm, W Vogel, C Ruiz, T Zellweger, M Svensson, O Andren, G Kristiansen, N Wernert, L Bubendorf, J Kirfel, S Biskup, S Perner. University Hospital, Bonn, Germany; University Hospital, Basel, Switzerland; St. Claraspital, Basel, Switzerland; University Hospital, Örebro, Sweden; University, Örebro, Sweden; Center for Genomics and Transcriptomics, Tuebingen, Germany.
Background: Castration resistant prostate cancer (CRPC) is the most aggressive form of prostate cancer (PCa) and remains a significant therapeutic challenge. The Mediator Complex is an evolutionarily conserved multi protein complex which is essential for the transcription of protein encoding genes and the regulation of diverse signaling pathways. The subunit MED12 is involved in the Wnt/ßCatenin pathway, which is increased or altered in advanced, hormone refractory PCa. The gene encoding *MED12* has recently been reported to be mutated in PCa. Therefore, the aim of our study was to investigate the role of MED12 and its relationship with ßCatenin in PCa and whether MED12 may serve as a novel target for therapeutic intervention for patients with CRPC.
Design: We have assessed the protein expression status of MED12 by immunohistochemistry (IHC) on a PCa progression cohort consisting of 110 locally defined PCa, 89 patients with primary PCa and 92 corresponding lymph node metastases, and 42 CRPC. In PCa cell lines, we performed *MED12* knockdown by siRNA followed by MTT proliferation assay. To investigate the effect of Wnt/ßCatenin signaling on the expression of MED12, the Wnt pathway was activated by treating cells with Lithium Chloride following western blot and qRT-PCR analysis for MED12.
Results: We found MED12 to show a strong nuclear overexpression in 40% of the CRPC, compared to a nuclear overexpression in only 10% of primary non-metastasized PCa, 0% of primary lymph node metastasized PCa, and 9% of lymph node metastases. Further, MED12 nuclear overexpression was significantly correlated with increased proliferative activity. In PCa cell lines, we showed that *MED12* knockdown decreases proliferation and that activation of Wnt/ßCatenin pathway leads to increased MED12 expression.
Conclusions: Our findings suggest that MED12 may be involved in promoting PCa cancer cell proliferation and survival in absence of androgens, and may serve as a novel target for therapeutic intervention for patients with CRPC.

1913 *MED15* Is Overexpressed at High Frequency in Head and Neck Squamous Cell Carcinoma and Is Implicated in TGFß Signaling

A Offermann, Z Shaikhibraim, M Braun, A Schrock, D Bohm, N Wernert, G Kristiansen, S Perner. University Hospital, Bonn, Germany.
Background: The Mediator Complex is an evolutionarily conserved multi protein complex which is essential for the transcription of protein encoding genes and the regulation of diverse signaling pathways. The subunit MED15 is essential for the TGFß pathway, which plays a major role in the pathogenesis of head and neck squamous cell carcinoma (HNSCC). In this study, we investigated the relevance of the Mediator subunit MED15 in tissues as well as in HNSCC cell lines. Furthermore we examined the relationship of MED15 with the TGFß pathway.
Design: MED15 expression level was determined by immunohistochemistry (IHC) and gene amplification/rearrangement status by Fluorescence In Situ Hybridization (FISH) on tissue microarrays (TMAs) comprising 719 HNSCC patients. For correlation studies, TMAs were assessed for the proliferation marker Ki67 as well as for pSMAD3 as an activation marker of the TGFß signaling by IHC. In several HNSCC cell lines, we performed *MED15* knockdown by siRNA as well as overexpression by a plasmid followed by proliferation assay. To investigate the role of MED15 upon TGFß signaling, we treated *MED15* -knockdown/ -overexpression cells with recombinant TGFß1/3 and evaluated the expression of TGFß target gene level by western blot and qRT-PCR. Furthermore, we determined whether TGFß signaling leads to increased expression of MED15 by treating cells with TGFß1/3.
Results: We found *MED15* to be overexpressed at high frequency in HNSCC tissues. MED15 overexpression correlates with Ki67 as a proliferation marker as well as with pSMAD3 as a marker of the TGFß signaling activation. Additionally, we found *MED15* to be amplified in HNSCC tissues as well as in two HNSCC cell lines. Knockdown or overexpression of *MED15* in the cell lines affects TGFβ signaling. Furthermore, we show that TGFβ signaling activation leads to increased expression of MED15 at protein level in HNSCC cell lines.
Conclusions: Our findings reveal a potential role of MED15 in HNSCC, and a direct implication with TGFß signaling which is known to play an important role in the pathogenesis of HNSCC.

1914 Are BCL2 and MYC Alterations Sufficient to Drive Lymphomagenesis?

RM Paolino, CL Robinson, TA Summers, DJ Hodson, LM Staudt. WRNMMC, Bethesda, MD; NCI/NIH, Bethesda, MD.
Background: Modern investigation of lymphomas has demonstrated that many can be characterized by the presence of recurrent genetic alterations such as chromosomal translocations targeting specific oncogenes. Prior to the development of more advanced techniques, these translocations were the sole abnormality detected in many lymphomas, suggesting they could be the primary lesion required for the development of the tumor. Lymphomas with alterations of both MYC and BCL2, so-called "double-hit" lymphomas, are associated with a far less favorable prognosis than those malignancies with only one of these translocations. Many have proposed that the combined alterations of these two genes are sufficient for human lymphomagenesis. To further elucidate the role of BCL2 and MYC, we infected primary human germinal center B-cells cultured *in vitro* with both MYC and BCL2 retroviruses.
Design: Germinal center B-cells were obtained from routine tonsillectomy specimens. These cells were cultured with fibroblasts engineered to express human CD40 ligand and in the presence of IL21. Cells were then infected with retrovirus containing either MYC or BCL2 coding sequence followed by an IRES and a stainable cell surface marker; CD4 or LyT2. Flow cytometric analysis of CD19, CD20, CD38, CD138, CD4 (MYC), and LyT2 (BCL2) was performed over time to monitor the relative expansion of single or double transduced cells along with their differentiation.
Results: Flow cytometric analysis performed on day 2 confirmed retrovirus infection but only a minority of cells expressed both MYC and BCL2. The B-cells expressing both BCL2 and MYC expanded to take over almost the entire population of cells within 10 days. However, shortly after this time point most cells cease dividing and lose expression of CD20. The immunophenotype ($CD19^+$, $CD38^+$, $CD20^-$, $CD138^-$) is different from typical double-hit lymphomas and suggests that these cells represent pre-plasmablasts.
Conclusions: The results suggest that, while mutations of both BCL2 and MYC do enhance B-cell proliferation and survival, this "double-hit" is not sufficient to transform human germinal center B cells cultured *in vitro*. These findings suggest that other genetic modifications, such as those emerging from next generation sequencing studies, may be additional requirements for human lymphomagenesis and may function to block differentiation and lock cells into a germinal center phenotype. We also propose to test combinations of these genetic hits to identify the minimum requirement for the *in vitro* transformation of human germinal center B cells.

1915 Collagen Expression Profiling of Normal and Diseased Human FFPE Tissues by Targeted Mass Spectrometry

AZ Rosenberg, AR Blackler, MR Emmert-Buck. National Cancer Institute, Bethesda, MD.

Background: Collagens are ubiquitously expressed proteins that account for approximately a third of all protein weight in the human body. They are a large protein superfamily encoded by 44 different genes and generally divided into eight different groups. Differential collagen expression is present both between tissues as well as within tissues (i.e., basement membranes versus interstitium). In benign tissues expression is relatively static and profiles are highly conserved between individuals, while in diseased states (such as cancer and sclerosing diseases) expression may be aberrant. However, due to extensive epitope redundancy, collagen subtyping using antibodies is challenging, and currently not feasible in a high-throughput manner. This property makes it difficult to identify the composite collagen makeup of any particular tissue. Multiple Reaction Monitoring (MRM) is one modality capable of addressing this complex problem.

Design: We have developed an MRM assay targeting unique peptides from 44 known human collagens and are profiling both normal and sclerosing tissues. All tissues used in the study were anonymized specimens obtained through an IRB approved NIH protocol. Formalin-fixed tissues were solubulized in denaturing buffer followed by tryptic digestion. For a disease state example, normal and sclerotic glomeruli were microdissected from FFPE kidney tissue. Labeled peptides were used for qualitative confirmation and quantitation.

Results: Examples of expression differences between two tissues included (but is not limited to) the differential expression of COL1A2, COL14A1 and COL23A1 (observed in testis) versus COL9A1 and COL18A1 in liver. Furthermore, we examined isolated normal and sclerotic kidney glomeruli and stroma. In sclerotic glomeruli we observed increased expression of COL6A3 and COL6A5 and decreased expression of COL3A1, COL6A1, COL6A2, and COL15A1. In sclerotic stroma there is increased expression in COL6A1, COL6A2 and COL6A3 and a decrease in the expression of COL3A1, and COL15A1. Thus in a single tissue undergoing sclerosing processes there are distinct collagen matrix profiles between compartments.

Conclusions: We describe a technique that allows for the multiplexed targeting of rare peptide species in complex protein digests derived from FFPE tissue for both qualitative and quantitative assessment. Using this approach we report a comprehensive and quantitative assay to look all known human collagens in FFPE and identify novel collagen profiles in diseased states.

1916 Platelet Cloaking of Cancer Cells Is a Universal Phenomenon

CD Spillane, NM Cooke, D Kenny, O Sheils, JJ O'Leary. Trinity College Dublin, Dublin, Ireland; The Coombe Women & Infants University Hospital, Dublin, Ireland; DCU, Dublin, Ireland; RCSI, Dublin, Ireland.

Background: Disseminated malignancy is responsible for the majority of cancer-related deaths and circulating tumour cells (CTCs) play a central role in metastasis. We and others have described the phenomenon of platelet cloaking of CTCs and how it induces an epithelial mesenchymal transition (EMT) signal in these cloaked cancer cells. A limitation of the current studies is the select number of cancer types that have been examined. In this study we aimed to determine if platelet cloaking of cancer cells is a universal phenomenon and whether the previously described EMT changes are a constant consequence of this interaction.

Design: The interaction between platelets and 14 *in vitro* human cancer cell lines of different origin and metastatic potential was examined. Platelet cloaking of each cell line was quantified by flow cytometry. The induction of an EMT was assessed by morphology analysis and by gene expression analysis of a panel of 10 EMT markers using RT-PCR.

Results: The results of this study demonstrate that platelet cloaking of cancer cells is a universal phenomenon occurring across all tumour types examined (breast, cervix, lung, melanoma, ovary, prostate and thyroid). The level of platelet adhesion varies significantly both across and within tumour types, ranging from 34% (C33a, primary cervical carcinoma) to 83% (SK-MES-1, metastatic lung squamous cell carcinoma). The effect of platelets on the epithelial phenotype of the cancer cells, again highlights the universal but heterogeneous nature with morphology changes akin to EMT observed at varying degrees across all cancer types. Data analysis the EMT marker panel expression levels supports the morphology results, with all cell lines having EMT-like changes. In line with the previous results overall there was no consistent pattern to the alterations, with the exception of plasminogen activator inhibitor 1 (PAI-1) where a highly significant and consistent increase was observed.

Conclusions: This is the first time the universal nature of the platelet cloaking phenomenon of cancer cells has been described. While the results of this study illustrate both the degree of physical interaction and subsequent downstream effects are heterogeneous, it does demonstrate similar dynamic processes are occurring. Understanding these processes could ultimately allow the establishment of therapies tailored to inhibiting metastasis, thus significantly reducing cancer morbidity rates.

1917 Platelets Enhance the Invasive Capabilities of Metastatic Ovarian Cancer *In Vitro*

CD Spillane, N Cooke, O Sheils, D Kenny, JJ O'Leary. Trinity College Dublin, Dublin, Ireland; The Coombe Women & Infants University Hospital, Dublin, Ireland; DCU, Dublin, Islamic Republic of Iran; RCSI, Dublin, Ireland.

Background: Ovarian cancer is the 5th leading cause of cancer related deaths in women. The poor survival rate is due to late stage diagnoses, with most patients asymptomatic until the disease has metastasised. Previously we described that there is a potent dynamic interaction between ovarian cancer cells and platelets *in vitro*, which involves platelet adhesion and activation. This in turn results in pro-survival, pro-angiogenic and epithelial mesenchymal transition (EMT) signals in the cancer cells. To further investigate these findings, the invasive capacity of cancer cells cloaked with platelets or platelets pre-treated with an anti-platelet agent (aspirin) was examined. As EMT has a role to play in cellular invasion, we also assessed the expression profile of EMT markers in these cloaked cancer cells.

Design: Cell lines 59M and SKOV3 were used as *in vitro* model systems of metastatic ovarian cancer. Cancer cells alone were compared to those incubated with platelets or with aspirin-treated platelets for 24hrs. To assess the capacity of cells to invade matrigel assays were used. Gene expression changes in EMT markers were determined by RT-PCR.

Results: The invasion of SKOV3 cells incubated with platelets was significantly greater ($p \leq 0.0001$) than SKOV3 cells alone. In contrast, platelets did not enhance invasion of the already highly invasive 59M cells. Aspirin significantly abrogated the platelet-mediated enhancement of invasion in SKOV3 cells ($p<0.05$). In SKOV3 cells incubated with platelets a significant loss in epithelial marker and increase in mesenchymal marker expression was observed, indicating the cells were undergoing EMT. Pre-incubation with aspirin did slightly abrogate this effect but did not reverse it. Platelets also induced EMT-like expression changes in 59M cells; however, in contrast there was only increases in expression of mesenchymal markers. The difference between the cell lines is potentially due to the significantly lower expression levels of the epithelial markers in 59M cells, this may in part explain the highly invasive nature of 59M.

Conclusions: These results demonstrate that platelets enhance the metastatic potential of ovarian cancer cells, with a concomitant induction of EMT. They also demonstrate for the first time that the antiplatelet agent aspirin attenuates this effect.

1918 Clinical Next Generation Sequencing (NGS) Identifies a Subset of Melanomas Harboring *SMARCB1* Mutations

DL Stockman, JL Curry, BR Russell, AJ Lazar, VG Prieto, MT Tetzlaff. University of Texas MD Anderson Cancer Center, Houston, TX.

Background: SMARCB1/INI1/BAF47/SNF5 is part of a complex that regulates gene expression through chromatin remodelling. SMARCB1 expression is lost or downregulated in multiple human tumor types, including epithelioid sarcoma, meningioma, epithelioid malignant peripheral nerve sheath tumor, and others. We describe three cases of melanoma with somatic mutations in *SMARCB1*.

Design: Clinical mutational analysis was performed in a CLIA-lab using a 46-gene NGS AmpliSeq™ Cancer Panel (Life Technologies, CA, USA). We searched our database to identify all cases of melanoma with mutations of SMARCB1. Immunohistochemistry for SMARCB1 was performed on tumor samples with anti-SMARCB1 mutation antibody (1:50; BAF47; BD Biosciences).

Results: Single-base substitutions in *SMARCB1* were detected in 3 cases of melanoma (Table 1) among ~765 melanoma samples analyzed to date (~0.4% of all samples) . Immunohistochemical studies demonstrated preservation of SMARCB1 protein expression in tumor cell nuclei of all cases. Clinical follow-up was available for all patients (median: 21 mos; range: 7-27 mos): all three patients were alive with regional metastases (at least one lymph node).

Clinicopathologic and mutational data

Case	1	2	3
Age/Gender	60/M	45/F	49/M
Location	Chest	Ear	Chest
Type	Nodular	Superficial Spreading Type	Superficial Spreading Type
Breslow (mm)	3.0	1.0	0.78
Mitoses (/mm2)	18	1	8
Ulceration	Present	Absent	Present
SMARCB1 Mutation	codon 160 (AAG to CAG) K160Q	codon 377 (CGT to CAT) R377H	codon 378 (CTT to TTT) L378F
Other mutations	BRAFV600E	TP53C238S	BRAFV600E; KITM541L
Metastases	Lymph node, lung	Lymph node	Lymph node
Follow up	AWD 21 mos	AWD 27 mos	AWD 7 mos

AWD: alive with disease

Conclusions: Single-base substitutions in *SMARCB1* are present in a subset of advanced melanomas with preserved SMARCB1 protein expression. Similar mutations have been described in other tumor types, where SMARCB1 is presumed to function as a tumor suppressor. Future studies are necessary to determine the possible diagnostic or therapeutic role of SMARCB1 in melanoma. These findings underscore the advantage of NGS platforms to expand the spectrum of tumors known to carry mutations in genes otherwise unexpected for a particular tumor type.

1919 Identification of Differentially Expressed miRNAs in Ovarian Cancer from Endometriosis in the Same Patient

R Wu, QF Ahmed, S Bandyopadhyay, B Alosh, E AbdulFatah, A Charestan, F Sarkar, R Ali-Fehmi. Wayne State University, Detroit, MI; Karmanos Cancer Institute, Detroit, MI.

Background: Endometriosis has a known association with ovarian cancer. The role of micro RNAs (miRNAs) as diagnostic and prognostic markers in ovarian cancer and endometriosis is unclear. The aim of this study was to recognize possible miRNAs in distinguishing ovarian cancer and endometriosis by comparing the miRNA profiling of ovarian cancer in patients with endometriosis.

Design: 19 cases of ovarian carcinoma with endometriosis in the same patient were identified. Of these 19 cases, 9 were endometrioid, 8 serous and 2 clear cell carcinoma. Microscopic foci of endometriosis and ovarian cancer were selected and macro-dissected. The miRNA expression profiling was performed initially from pooled RNA samples from ovarian cancer and endometriosis from all cases through LC Sciences using array technology. Later, the abnormal expression of selected miRNAs was validated in individual cases by quantitative real-time PCR (qRT-PCR).

Results: The miRNA profiling demonstrated deregulation of over 1000miRNAs in ovarian cancer of which, the top seven were further validated by qRT-PCR. The expression of tumor suppressor miRNAs miR-1, miR-133a, and miR-451 were reduced significantly in ovarian cancer while expression of the oncogenic miRNAs

miR-141, miR-200a, miR-200c, and miR-3613 was elevated significantly in ovarian cancer. Conversely, miRNAs for oncogene and tumor suppressor gene expression in endometriosis showed a reverse trend as shown in Figures 1 and 2.

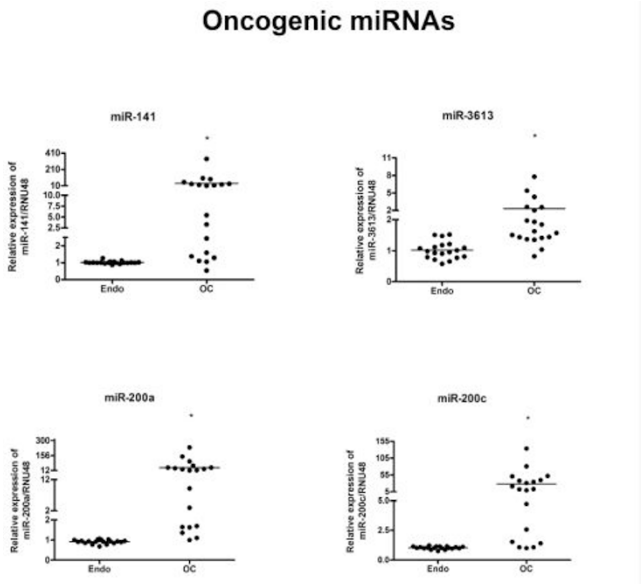

Figure 1: Oncogenic miRNAs were significantly increased in OC (ovarian cancer) Compared to respective Endo (endometriosis) * p < 0.05

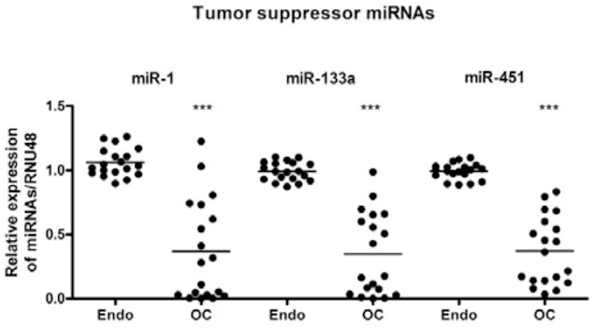

Figure 2 : Tumor suppressor miRNAs were significantly reduced in OC (ovarian cancer) Compared to respective Endo (endometriosis) *** p < 0.0001

Conclusions: There are significant differences between ovarian cancer and its associated endometriosis at the level of miRNA transcription. Both tumor suppressor miRNA (1, 133a, 451) and oncogenic miRNAs(141, 200a, 200c, 3613) are possible molecules that distinguish ovarian cancer from its associated endometriosis. These miRNAsshould be studied further to identify their role as possible biomarkers in the development of ovarian cancer in patients with endometriosis.

1920 Distribution of Mutagenic RNA:DNA Hybrids in Precancerous Lesions and Solid Malignancies

RR Xian, V Cikes-Culic, M Vujevic, AE Ross, M Vuica-Ross. Johns Hopkins Hospital, Baltimore, MD.

Background: Accumulation of DNA damage in the form of point mutations and chromosomal abnormalities in tumors is a well-documented phenomenon. Less is known about how these changes are generated. DNA structural abnormalities such as faulty transcription and replication-associated RNA:DNA hybrids are one of the major sources of double strand breaks in lower level organisms. However, the role of these RNA:DNA hybrids in mammalian tumorigenesis is unknown.

Design: Using tissue array technology we examined RNA:DNA hybrid formation, expression of the hybrid repair protein, RNASEH2A, and expression of the DNA damage response protein YH2AX in a broad range of normal tissues, benign lesions and malignant lesions. Immunohistochemical labeling was scored using the HistoScore scheme that takes into consideration area and intensity of labeling.

Results: Unlike normal tissues, which are devoid of any detectable RNA:DNA hybrids (0/6 bladders, 0/2 breasts, 0/5 prostates), a large fraction of benign lesions and early cancerous lesions are immunoreactive for RNA:DNA hybrids (16/30 bladder hyperplasia, 1/3 bladder papillomas, 16/30 non-metastatic bladder carcinoma, 16/38 prostate hyperplasia, 2/2 Prostatic Intraepithelial Neoplasia, 22/24 non-metastatic prostate carcinoma, 19/30 benign breast lesions, 18/31 non-metastatic breast carcinoma). Interestingly, the presence of these hybrids in metastatic cancer is relatively infrequent (1/3 metastatic bladder carcinoma, 0/6 metastatic breast carcinoma, 8/16 metastatic prostate carcinoma). The distribution of the DNA damage response protein YH2AX, which is a marker of double strand DNA breaks, closely follows the distribution of RNA:DNA hybrids (22/27 bladder lesions with hybrids, 25/48 prostate lesions with hybrids). In contrast, RNASEH2A is only upregulated in metastasis (2/3 metastatic bladder carcinoma, 12/16 metastatic prostate carcinoma), and in a small subset of non-metastatic cancers (9/30 bladder carcinoma, 8/24 prostate carcinoma). RNASEH2A is completely absent from normal tissues, benign lesions, and precancerous lesions.

Conclusions: RNA:DNA hybrids are frequently found in precancerous lesions and in early stage malignancies, while the RNA:DNA hybrid repair protein, RNASEH2A, is overexpressed predominantly in metastatic cancers. This suggests that RNASEH2A acts as a non-oncogene addiction gene that maintains the survival of aggressive tumors in the setting of increased cellular stress by repairing DNA structural abnormalities such as RNA:DNA hybrids. Our findings point to RNASEH2A as a potential novel target in preventing and treating aggressive malignancies.

1921 Pathobiologic Significance of Molecular Analysis and Clinical Findings and Their Relationship with Mucin Status in FNA of Pancreatic Cysts

J Xie, B Corcoran, S Finkelstein, JF Silverman. Allegheny General Hospital, Pittsburgh, PA; RedPath Integrated Pathology, Inc, Pittsburgh, PA.

Background: Pancreatic cyst (PC) fluid cytology analysis can be challenging for a definitive diagnosis. Microscopic examination of PC fluid primarily targets cytologic atypia/dysplasia; however, the presence of mucin is believed to be an important feature. We evaluated the mucin status of PC and correlated the findings with the presence of free DNA, molecular abnormalities, biochemical analysis, clinical findings and FNA cytologic examination.

Design: A consecutive series of 608 indeterminate PC needle aspirates were retrospectively evaluated. EUS findings assessed as potentially aggressive features included PC size ≥3 cm, duct dilation ≥1 cm or solid component formation. CEA levels >192 ng/ml were indicative of mucinous cyst formation; levels >1000 ng/ml were concerning for aggressive mucinous PC biology. Molecular analysis performed on original cyst fluid targeted 3 parameters associated with positive mucin status and potentially aggressive disease: 1) high DNA concentration, 2) oncogene point mutations of KRAS and/or GNAS and 3) the presence of multiple tumor suppressor gene loss assessed by loss of heterozygosity (LOH) in a 24-marker panel. Combined molecular and clinical findings associated with aggressive biology was used to classify the PC as 'high risk'.

Results: The relationship of clinical and molecular findings to the mucin status is shown in the Table. Clinical and molecular parameters associated with aggressive biology in PC disease were equivalent between the mucin+ and mucin- groups and are not statistically significant (P>0.05, Chi Square test).

Table

	Mucin + %	Mucin - %
Cyst size ≥ 3cm	17	17
Duct dilation ≥ 1cm	3	2
Solid component formation	10	14
CEA level 192-1000 ng/ml	21	20
CEA level >1000 ng/ml	23	26
High DNA concentration	18	20
KRAS mutation	23	26
GNAS mutation	4	4
Multiple LOH mutations	6	4
'High Risk' by integrated clin/mol	13	14

The case numbers of mucin + and mucin - are 421 and 187, respectively.

Conclusions: 1) The pathobiologic significance of mucin in the cytology smears should not necessarily be regarded as evidence of aggressive disease; 2) Mucin in cytologic smears did not have significant correlation with high level CEA; 3) Molecular abnormalities are present in cysts lacking mucin and can represent high risk of aggressive disease.

1922 MiRNA137 Mimics Targeting MCL-1 as a Novel Therapeutic Agent in Preclinical Models of Multiple Myeloma

Y Yang, MN Saha, Y Chen, H Chang. University Health Network, Toronto, ON, Canada.

Background: Deregulated expression of miRNAs has shown to play an important role in the pathogenesis of multiple myeloma (MM). Since miRNAs can act as a oncogenes or tumor suppressor genes, a promising therapeutic strategy by targeting the miRNA regulatory network is to enforce the expression of miRNAs that act as tumor suppressor genes in MM.

Design: We investigated miR-137 expression patterns by RT-qPCR in MM cell lines and primary diagnostic MM patient samples, as well as immunobloting analysis for the targeted gene protein expressions. To determine miR-137 functional effect on antimyeloma activity in vivo, MM. 1S cells were transducted with lentivirus-based miR-137 for stable enforced expression cell line, and investigated in SCID mouse xenograft model of MM. In addition, lipidic-formulated synthetic miR-137 was carried out in SCID model to evaluate the efficacy on anti-MM.

Results: Examination of the basal expression level of miR-137 in MM patient tumor cells and MM cell lines showed that miR-137 expression was significantly lower compared to normal plasma cells and peripheral blood mononuclear cells from healthy donors. We found overexpression of miR-137 resulted in reduction of MCL-1, an anti-apoptotic protein expressions, as well as alteration of proapoptotic genes, and induction of cell death and apoptosis. Moreover, transient overexpression of miR-137 in MM.1S cells significantly decreased the number of colonies and the number of migrating cells. In contrast, overexpression of MCL-1 consecutively reduced the effect of miR-137 on MM cells. Importantly, lentiviral vector-transduced MM xenografts with constitutive miR-137 expression showed tumor growth was significantly inhibited in SCID mice, and prolonged mice survival. The similar results were obtained that mouse tumor progression was retarded, and survival was improved while received intratumoral

injections with lipidic-formulated synthetic miR-137. Moreover, immuno-blotting and -staining analysis of tumor tissue demonstrated that MCL-1was decreased in miR-137 overexpressing tumors compared to vector or delivery regent controls, as well as reduced Ki67 and increased Tunnel activities.
Conclusions: Our findings provide a proof-of-principle that lentivirus-based miR-137 or formulated synthetic miR-137 exerts therapeutic activity in preclinical models and support a framework for development of miR-137based treatment strategies in MM patients.

1923 Mining TCGA/COMSIC Data Reveals Rationale of Expanding Molecular/Genetic Testing to More Tumor Types: Implications for Personalized Oncology

H Zhong. Rutgers Robert Wood Johnson Medical School and Rutgers Cancer Institute of New Jersey, New Brunswick, NJ.
Background: Molecular/genetic testing has become a daily routine for pathology. Examples include PCR or FISH based analyses for ERBB2, BRAF, KRAS, EGFR, ALK and KIT. Results from the tests permit genomic classification of solid tumors and determine further managements. However, the current routine aims only to the most common tumor types based on prior translational studies. Large-scale cancer genomic data are gradually accumulated and are now available to research communities. Information from the large-scale well-maintained datasets may change our original concepts on cancer biology and genomics.
Design: TCGA cBioPortal for Cancer Genomics was used as an initial source of data mining. Tumors with genetic alterations of a specific gene in greater than 10% cases were recorded, arbitrarily designated as high-frequency alteration. COSMIC database was then queried if known activating mutation could be identified on the tumor.
Results: High-frequency genetic alteration on ERBB2 was demonstrated in four different carcinomas including breast and gastric carcinoma. Various tumors were shown to have high-frequency alteration on BRAF, KRAS and EGFR. ALK gene was altered in 10% cutaneous melanomas in addition 11.6% lung adenocarcinomas. Only one non-GIST tumor, glioblastoma, showed high-frequency KIT alteration while the majority were amplification. Below table shows examples.

Examples of Genetic Alterations in Solid Tumors

Gene	Tumor	Amplification (%)	Deletion (%)	Mutation (%)	Mixed Altera-tions (%)	Total Altera-tions (%)	Total Case Tested
ERBB2	Urothelial carcinoma	3.8		11.5	3.8	19.1	26
	Breast invasive carcinoma	13.6		1.4	0.1	15.1	760
	Endometrioid carcinoma	7.1		3.3		10.4	240
BRAF	Colorectal adenocarcinoma	0.5		10		10.5	221
	Lung adenocarcinoma	1.6		9.3	0.8	11.7	129
	Ovarian serous cystadenocarcinoma	10.6	0.3	0.6		11.5	311
	Cutaneous melanoma	0.9	0.4	45.2	6.1	52.6	228
	Thyroid carcinoma		0.3	58.9		59.2	319
EGFR	Glioblastoma	32.2		4.7	23.7	60.6	236
	Head & neck squamous cell carcinoma	8.6	0.3	3	1.7	13.6	302
	Lung adenocarcinoma	1.6		13.2	3.8	18.6	182
	Gastric adenocarcinoma	5.5	0.5	5		11	219

Conclusions: It is reasonable to extend PCR or FISH based analyses on all late-stage tumors with high-frequency of specific genetic alterations. At least, available immunohistochemistry should be performed to select candidates for further target genetic testing. By doing so, more cancer patients may access to personalized management before next-generation sequencing is adopted as a clinical routine.

Pediatric Pathology

1924 Fine Needle Aspiration Cytology in Pediatric Bone and Soft Tissue Spindle Cell Lesions

N Bures, L Pantanowitz, SE Monaco. University of Pittsburgh Medical Center, Pittsburgh, PA.
Background: Spindle cell lesions in children can be difficult to characterize by fine needle aspiration (FNA) given that the differential diagnosis varies by age, and includes reactive tumor-like lesions as well as benign and malignant neoplasms. The objective of this study is to assess the diagnostic utility of FNA in the diagnosis of spindle cell lesions in the pediatric population.
Design: Spindle cell lesions in patients 22 years of age or less were identified during the time period from 2006 to 2012. Cytology cases and surgical cases with a prior FNA were included. Patient demographics, FNA diagnosis, ancillary studies and available follow-up were investigated and correlated.
Results: A total of 18 cases were identified in patients ranging from 7 weeks to 22 years of age, including 9 males and 9 females. Lesions included 14 (78%) soft tissue and 4 (22%) bone lesions. Samples were acquired by image-guided FNA (9; 50%) or palpation guided FNA (9; 50%). Thirteen (72%) cases had corresponding histopathology. Four (22%) cases had sufficient material for ancillary studies. Table 1 shows the correlation of cytology adequacy and diagnoses with histological follow-up. No false positive diagnoses were identified.

Table 1. Cytohistological Correlation in Pediatric Spindle Cell Lesions

FNA Adequacy & Diagnosis	No. of cases (%)	No. with histological follow-up (%)	Histopathology Diagnosis Reactive	Histopathology Diagnosis Benign Neoplasm	Histopathology Diagnosis Malignant Neoplasm
Unsatisfactory, Non-Diagnostic	6 (33%)	3 (50%)	0	1 (hemangioma)	2 (osteosarcoma)
Less than optimal, Negative	2 (11%)	1 (50%)	0	1 (hemangioma)	0
Less than optimal, Atypical or Suspicious	2 (11%)	2 (100%)	0	1 (fibromatosis)	1 (epithelioid sarcoma)
Satisfactory, Atypical or Suspicious	3 (16%)	3 (100%)	0	3 (solid aneurysmal bone cyst, localized tenosynovial giant cell tumor, desmoplastic fibroma)	0
Satisfactory, Positive for Neoplasm	5 (28%)	4 (80%)	0	3 (schwannoma, ganglioneuroma, myofibroma)	1 (high-grade sarcoma NOS)

Conclusions: In conclusion, FNA is useful to triage pediatric spindle cell lesions, in that it can usually exclude more common lymphoid lesions and small round blue cell tumors, thereby directing further management. However, obtaining sufficient material for full characterization with ancillary studies can be difficult, and thus, maximizing cell block material or using concurrent core biopsy can be helpful. Neoplasms that are particularly difficult to diagnose on FNA due to low cellularity were hemangioma and osteosarcoma.

1925 Thyroid Carcinoma in Children and Adolescents: An Institutional Review

NTT Can, T Antic, JB Taxy. University of Chicago, Chicago, IL; NorthShore University HealthSystem, Evanston, IL.
Background: Papillary thyroid cancer (PTC) is the most common thyroid malignancy in children. The diffuse sclerosing (DSV) and cribriform morular (CMV) variants have specific clinical and pathologic associations. DSV is associated with thyroiditis, diffuse growth pattern, and *RET* mutations; while CMV is associated with familial adenomatous polyposis (FAP), a gross mass, and *APC* mutations. This study reviews pediatric thyroid carcinomas.
Design: The files at University of Chicago yielded 43 thyroid carcinomas (total or partial thyroidectomy specimens) in patients <20 years from January 2005 to October 2012.
Results: There were 34 total and 9 partial thyroidectomies among 11M:32F (ages 7-20 years; mean: 16.2 years). PTC distribution was as follows: 18 classic, 15 DSV, 4 follicular variant, and 2 CMV. Other subtypes of thyroid carcinoma included 2 minimally invasive follicular, 1 medullary, and 1 Hurthle cell carcinoma. DSV cases were multicentric (11 cases) with both diffuse growth (3 cases) and mass formation (12 cases), squamous metaplasia (11 cases), psammoma bodies (14 cases), and background thyroiditis (15 cases). In CMV cases, there was the addition of cribriform proliferations without background thyroiditis. One CMV case was sporadic (without β-catenin nuclear positivity by immunohistochemistry); the other was FAP-related with β-catenin nuclear positivity by immunohistochemistry and confirmed germ-line *APC* mutation. When compared with classic PTC, DSV was more frequently associated lymph node metastases ($p<0.001$) and advanced TNM (III or IV) stage ($p=0.004$). The only death in this series occurred in a patient with DSV.
Conclusions: This series shows DSV as the major PTC subtype in the pediatric group. Though diffuse growth has been reported as characteristic of DSV, 12 cases exhibited a gross mass. Squamous metaplasia, psammoma bodies, background thyroiditis, and multicentricity were common histologic features. The histological features shared between DSV and CMV suggest they may be part of a morphologic spectrum. In the absence of cribriform proliferations, DSV and CMV can appear morphologically identical. Molecular diagnostics may aid in distinguishing these two entities. While the association between CMV and FAP is well known, some cases of CMV may be sporadic. An example of each was encountered in this series. DSV has been previously identified as an aggressive PTC variant and accounted for the only death in this series. Histologic subtype and tumor stage may be significant determinants of the biologic behavior of thyroid cancer in children.

1926 MiR-125b in Pediatric Fibroblastic Tumors

R Cappellesso, F Simonato, L Iaria, A Fassina, L Ventura, A Zin, R Alaggio. University of Padova, Padova, Italy.
Background: Intermediate and malignant fibroblastic-myofibroblastic tumors are an important group of malignancies that includes variants of fibrosarcoma, such as congenital infantile fibrosarcoma (CIFS), primitive myxoid mesenchymal tumor of infancy (PMMTI), and undifferentiated sarcoma (US). To date, little is known about the involvement of microRNAs in these tumors. MiR-125b regulates cellular quiescence (reversible cell-cycle arrest) and has been reported to be up-regulated in quiescent fibroblasts. However, the down-regulation of miR-125 has been reported in several tumors where it exhibits tumor suppressor properties, while its over-expression in other malignancies has been related to oncogene functions.
Design: MiR-125b expression was analysed by using qRT-PCR in formalin-fixed paraffin-embedded specimens of 6 CIFSs with known ETV6-NTRK3 gene fusion, 6 sarcomas without this genetic alteration (3 PMMTIs and 3 USs), and 7 cutaneous scars (negative controls). Statistical analysis was done using Student *t*-test.